Application of Conservation Laws with Source Terms to the Shallow Water Equations and Crowd Dynamics

Polly Smith

September 2004

Abstract

In this dissertation we look at the application of two dimensional conservation laws with source terms to two specific physical examples, the shallow water equations and crowd flow. There are a number of techniques that can be used to numerically approximate such systems. We discuss the Q scheme method of Bermúdez & Vázquez, focusing on an extension to Roe's Q scheme. The technique of dimensional splitting is used to decompose the systems into two one-dimensional problems that are solved alternately in the x and y directions. For the shallow water equations we examine two different test problems. We begin by considering a non-rotating frame of reference, before extending the equations to include the effects of the Earth's rotation. The β-plane approximation is used to avoid the complications of spherical geometry whilst retaining the leading order effect of the Earth's curvature. We then move on to develop a two dimensional macroscopic model of crowd flow based on a one-dimensional continuum model proposed by Payne and Whitham. The equations are transformed into a system of conservation laws, with source term in the form of a relaxation term. A series of numerical experiments are used to evaluate the accuracy of the model.

Declaration

I confirm that this is my own work and the use of all materials from other sources has been properly and fully acknowledged.

Signed

Polly Smith

September 2004

Acknowledgements

Firstly, I would like to thank my supervisor Professor Mike Baines for his continual help and support throughout this project. His patience and humour is admirable. I am also very grateful to the postgraduate secretary Sue Davis and my fellow MSc students for their support and encouragement over the past year.

Apologies go to my family for all the angst - thank you for your tolerance. A big thank you to all my friends for always being there despite my neglect, and to Tim for listening to my worries.

Many thanks to the NERC for their generous financial support.

Contents

Chapter 1

Introduction

Hyperbolic systems of conservation laws with source term arise naturally in a wide variety of applications. Many practical problems in science and engineering involve mathematical models based on this type of system. In two space dimensions the equations take the form

$$\frac{\partial \mathbf{w}}{\partial t} + \frac{\partial \mathbf{F}(\mathbf{w})}{\partial x} + \frac{\partial \mathbf{G}(\mathbf{w})}{\partial y} = \mathbf{R},$$

where $\mathbf{w}$ is a vector of conserved quantities, $\mathbf{F}(\mathbf{w})$ and $\mathbf{G}(\mathbf{w})$ are functions representing the physical flux, and $\mathbf{R}$ is a source term. Often, the flux functions are nonlinear functions of $\mathbf{w}$, leading to nonlinear systems of partial differential equations (PDEs). Some of these systems have exact solutions, but generally analytical solutions to these problems are not available since they are extremely difficult, if not impossible, to find. Thus we seek to devise numerical methods for their approximate solution. Indeed, the significance of these equations to a number of important fields has provoked increasing research in recent years.

In this project we look at the application of conservation laws with source

term in two dimensions by considering two physical examples - The shallow water equations and crowd dynamics. Many similarities exist between the flow of crowds and that of a shallow fluid. The movement of a large crowd exhibits many of the attributes of a fluid and macroscopic pedestrian models utilise this analogy by treating the crowd as a continuum. There are, however, drawbacks to this assumption as unlike a fluid, a crowd has the ability to think and will react to it surroundings.

Chapter 2 introduces the numerical method that will be used to solve the two dimensional hyperbolic systems of equations arising from the shallow water and crowd models. In chapter 3 we derive the shallow water equations for two dimensional, incompressible, irrotational flow in a rectangular channel and apply the approach discussed in Chapter 2 to the model. We then extend the model to include the effects of the Earth's rotation by introducing a coriolis parameter f and using the β-plane approximation to avoid the complications of spherical geometry. Two test cases are presented, the results from which are shown. In chapter 4 we consider a two dimensional extension to the Payne-Whitham model for crowd flow. A series of numerical trials are used to assess the performance of the model, looking at the two dimensional case of a crowd moving towards an exit in a room. Finally, in chapter 5 we outline the conclusions that can be drawn from this study and propose areas for development and possible further study.

Chapter 2

Numerical Methods

There are a number of techniques that can be used to numerically approximate the two dimensional system of conservation laws with source term

$$\frac{\partial \mathbf{w}}{\partial t} + \frac{\partial \mathbf{F}(\mathbf{w})}{\partial x} + \frac{\partial \mathbf{G}(\mathbf{w})}{\partial y} = \mathbf{R}, \tag{2.1}$$

such as finite element, finite volume and finite difference methods. In this chapter we use the approach of dimensional splitting to derive a second order accurate scheme that can be used to solve systems of the type (2.1). We then introduce the Q Schemes of Bermúdez & Vázquez [1] and explain how they can be used to give expressions for the numerical flux and numerical source terms. Finally, we consider the specific example of Roe's Q Scheme.

2.1 Dimensional Splitting

The method of dimensional splitting was first proposed by Yanenko [20].

By rewriting the source term as

$$\mathbf{R} = \mathbf{f} + \mathbf{g},$$

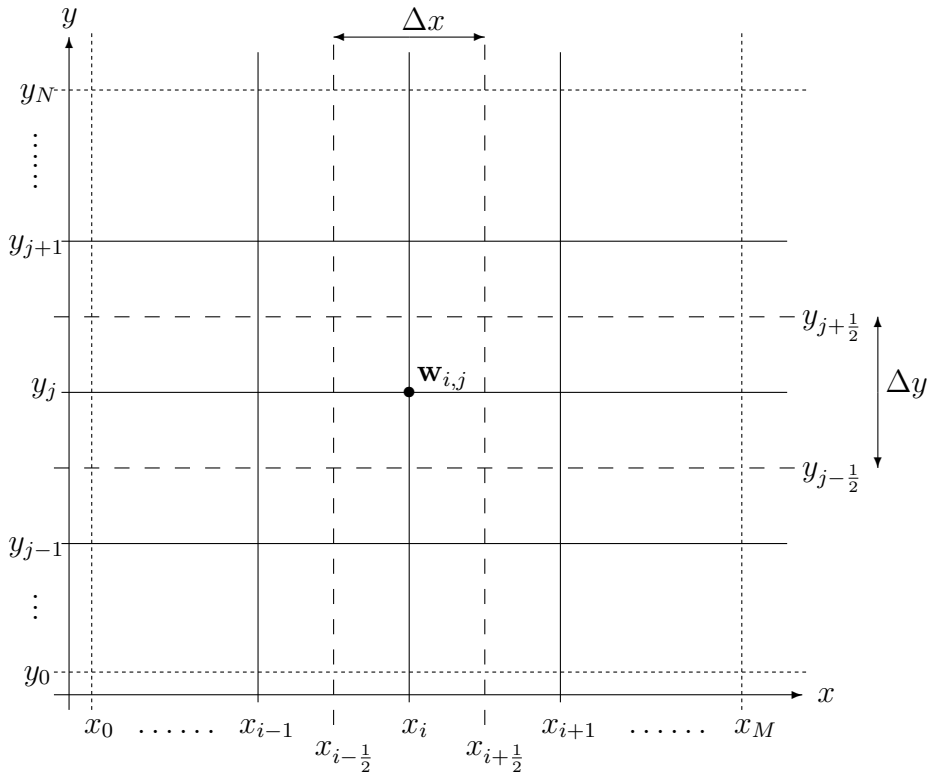

Figure 2.1: The computational grid

(where the vectors $\mathbf{f}$ and $\mathbf{g}$ contain the x and y direction components of $\mathbf{R}$ respectively) we can decompose the two dimensional system (2.1) into two parts,

$$\frac{1}{2}\frac{\partial \mathbf{w}}{\partial t} + \frac{\partial \mathbf{F}(\mathbf{w})}{\partial x} = \mathbf{f} \tag{2.2}$$

and

$$\frac{1}{2}\frac{\partial \mathbf{w}}{\partial t} + \frac{\partial \mathbf{G}(\mathbf{w})}{\partial y} = \mathbf{g}. \tag{2.3}$$

We begin by discretising the domain on a cartesian mesh, see Figure 2.1. The numerical solution is denoted by $\mathbf{w}_{i,j}^n \approx \mathbf{w}(i\Delta x, j\Delta y, n\Delta t)$, where Δt is the temporal step length, Δx and Δy are the spatial step sizes in the x and y

directions respectively and $\mathbf{F}^*_{i+\frac{1}{2}}$ and $\mathbf{G}^*_{i,j+\frac{1}{2}}$ are the corresponding numerical flux functions. $\mathbf{R}^*_{i,j}$ is a numerical source function taken to be of the form

$$\mathbf{R}^*_{i,j} = \mathbf{f}^*_{i,j} + \mathbf{g}^*_{i,j}$$

where $\mathbf{f}^*_{i,j}$ and $\mathbf{g}^*_{i,j}$ are the source term approximations containing the x and y direction components only.

The boundaries are given by the lines $(x_{-\frac{1}{2}}, y_j)$, $(x_{M+\frac{1}{2}}, y_j)$, $(x_i, y_{-\frac{1}{2}})$ and $(x_i, y_{N+\frac{1}{2}})$ where M and N denote the number of intervals in the x and y directions respectively. Numerical boundary conditions are required at each of these points and will be discussed in more detail later both for the shallow water equations and crowds.

The simplest form of splitting then discretises in two steps. First, we solve in the x coordinate direction using a half time step $\frac{\Delta t}{2}$ to obtain an approximation of (2.2), $\mathbf{w}^{n+\frac{1}{2}}$,

$$\mathbf{w}^{n+\frac{1}{2}}_{i,j} = \mathbf{w}^n_{i,j} - \frac{\Delta t}{2\Delta x}\left(\mathbf{F}^*_{i+\frac{1}{2},j} - \mathbf{F}^*_{i-\frac{1}{2},j}\right) + \frac{\Delta t}{2\Delta x}\mathbf{f}^*_{i,j}.$$

This is then used as the initial conditions for approximating (2.3) using a half time step to obtain $\mathbf{w}$ at the next time level t^{n+1},

$$\mathbf{w}^{n+1}_{i,j} = \mathbf{w}^{(n+\frac{1}{2})}_{i,j} - \frac{\Delta t}{2\Delta y}\left(\mathbf{G}^{*(n+\frac{1}{2})}_{i,j+\frac{1}{2}} - \mathbf{G}^{*(n+\frac{1}{2})}_{i,j-\frac{1}{2}}\right) + \frac{\Delta t}{2\Delta y}\mathbf{g}^{*(n+\frac{1}{2})}_{i,j}.$$

However, this scheme is only first order accurate in time. Strang [15] derived a second order accurate approach by discretising in three steps, (2.2) is solved using a quarter time step, $\frac{\Delta t}{4}$. The values $\mathbf{w}^{(n+\frac{1}{4})}_{i,j}$ are then used as initial conditions for (2.3) which is approximated using a half time step, $\frac{\Delta t}{2}$. Finally, we solve again in the x direction using a quarter time step and $\mathbf{w}^{(n+\frac{3}{4})}_{i,j}$ as

initial conditions to obtain $\mathbf{w}^{n+1}$.

$$\mathbf{w}_{i,j}^{n+\frac{1}{4}} = \mathbf{w}_{i,j}^{n} - \frac{\Delta t}{4\Delta x}\left(\mathbf{F}^{*}_{i+\frac{1}{2},j} - \mathbf{F}^{*}_{i-\frac{1}{2},j}\right) + \frac{\Delta t}{4\Delta x}\mathbf{f}^{*}_{i,j}$$

$$\mathbf{w}_{i,j}^{n+\frac{3}{4}} = \mathbf{w}_{i,j}^{(n+\frac{1}{4})} - \frac{\Delta t}{2\Delta y}\left(\mathbf{G}^{*(n+\frac{1}{4})}_{i,j+\frac{1}{4}} - \mathbf{G}^{*(n+\frac{1}{4})}_{i,j-\frac{1}{2}}\right) + \frac{\Delta t}{2\Delta y}\mathbf{g}^{*(n+\frac{1}{4})}_{i,j},$$

$$\mathbf{w}_{i,j}^{n+1} = \mathbf{w}_{i,j}^{(n+\frac{3}{4})} - \frac{\Delta t}{4\Delta x}\left(\mathbf{F}^{*(n+\frac{3}{4})}_{i+\frac{1}{2},j} - \mathbf{F}^{*(n+\frac{3}{4})}_{i-\frac{1}{2},j}\right) + \frac{\Delta t}{4\Delta x}\mathbf{f}^{*(n+\frac{3}{4})}_{i,j}.$$

2.1.1 Stability

A *necessary* condition for the stability of a homogeneous system of equations

$$\frac{\partial \mathbf{w}}{\partial t} + \frac{\partial \mathbf{F}(\mathbf{w})}{\partial x} = 0,$$

is

$$max_i|\lambda_k^F \frac{\Delta t}{\Delta x}| \leq \nu. \tag{2.4}$$

where λ_k^F are the eigenvalues of the Jacobian matrix $\mathbf{A}$ and ν is a bound constant known as the Courant or CFL number (after Courant, Friedrichs and Lewy).

In this instance we have two stability conditions, (2.4) for the x direction and

$$max_j|\lambda_k^G \frac{\Delta t}{\Delta y}| \leq \nu. \tag{2.5}$$

for the y direction. To ensure that both (2.4) and (2.5) are satisfied and that the dimensional splitting scheme remains stable we choose our time step Δt such that

$$\Delta t \leq \frac{min(\Delta x, \Delta y)}{max_{i,j}(|\lambda^F|, |\lambda^G|)} \quad .$$

2.2 Q Schemes

In this section we discuss a numerical technique proposed by Bermúdez & Vázquez [1] for approximating two dimensional hyperbolic systems of conservation laws with source term.

In [1] Bermúdez & Vázquez introduce a general class of upwind methods for solving nonhomogeneous problems. They propose extensions to a number of well known and well studied flux difference and flux splitting techniques using an upwinded discretisation of the source term. In particular, a class of upwind schemes known as Q schemes are considered. The schemes were implemented using a simple first order explicit finite difference scheme

$$\mathbf{w}_{i,j}^{n+1} = \mathbf{w}_{i,j}^{n} - \frac{\Delta t}{\Delta x}\left(\mathbf{F}^{*}_{i+\frac{1}{2},j} - \mathbf{F}^{*}_{i-\frac{1}{2},j}\right) + \Delta t \mathbf{R}^{*}_{i,j}.$$

Although the paper only considers problems in one space dimension it is noted that the proposed techniques can be extended to multi-dimensional problems. Due to the nature of this study we will present the method in terms of two dimensions. This can then be combined with the dimensional splitting discussed above to obtain a method that is second order accurate.

Q schemes are a family of upwind schemes corresponding to numerical flux functions of the form

$$\mathbf{F}^{*}_{i+\frac{1}{2},j} = \frac{1}{2}\left(\mathbf{F}^{n}_{i,j} + \mathbf{F}^{n}_{i+1,j}\right) - \frac{1}{2}|\mathbf{Q}^{n}_{i+\frac{1}{2},j}|\left(\mathbf{w}^{n}_{i+1,j} - \mathbf{w}^{n}_{i,j}\right), \tag{2.6}$$

and

$$\mathbf{G}^{*}_{i,j+\frac{1}{2}} = \frac{1}{2}\left(\mathbf{G}^{n}_{i,j} + \mathbf{G}^{n}_{i,j+1}\right) - \frac{1}{2}|\mathbf{Q}^{n}_{i,j+\frac{1}{2}}|\left(\mathbf{w}^{n}_{i,j+1} - \mathbf{w}^{n}_{i,j}\right), \tag{2.7}$$

The matrix $\mathbf{Q}$ depends continuously on $\mathbf{w}_L$ and $\mathbf{w}_R$ and is characteristic of each Q scheme.

Bermúdez & Vázquez [1] propose upwinding the source term in a similar manner to the flux. The numerical source functions $\mathbf{f}^*$ and $\mathbf{g}^*$ are taken to be of the form

$$\mathbf{f}^*_{i,j} = \mathbf{f}^*_{i+\frac{1}{2},j} + \mathbf{f}^*_{i-\frac{1}{2},j} \quad \text{and} \quad \mathbf{g}^*_{i,j} = \mathbf{g}^*_{i,j+\frac{1}{2}} + \mathbf{g}^*_{i,j-\frac{1}{2}}. \tag{2.8}$$

The left and right numerical sources $\mathbf{f}^*_{i-\frac{1}{2},j}$, $\mathbf{f}^*_{i+\frac{1}{2},j}$ are obtained by projecting the source term onto the eigenvectors of $\mathbf{Q}$ to give

$$\mathbf{f}^*_{i-\frac{1}{2},j} = \frac{1}{2}\left[\mathbf{I} + |\mathbf{Q}|\mathbf{Q}^{-1}\right]_{i-\frac{1}{2},j} \hat{\mathbf{f}}_{i-\frac{1}{2},j} \tag{2.9}$$

and

$$\mathbf{f}^*_{i+\frac{1}{2},j} = \frac{1}{2}\left[\mathbf{I} + |\mathbf{Q}|\mathbf{Q}^{-1}\right]_{i+\frac{1}{2},j} \hat{\mathbf{f}}_{i+\frac{1}{2},j} \tag{2.10}$$

where $\hat{\mathbf{f}}$ represents an approximation of $\mathbf{f}$. Expressions for $\mathbf{g}^*$ are obtained by symmetry.

$|\mathbf{Q}|$ can be obtained by using

$$|\mathbf{Q}| = \mathbf{X}^{-1}|\mathbf{\Lambda}|\mathbf{X}$$

where $\mathbf{\Lambda}$ represents a matrix whose diagonal elements are the eigenvalues of $\mathbf{Q}$, and $\mathbf{X}$ is a matrix containing the right eigenvectors.

Note that since

$$\mathbf{f}^*(\mathbf{w}_L, \mathbf{w}_R) \longrightarrow \mathbf{f}(\mathbf{w}) \quad \text{as} \quad \mathbf{w}_L, \mathbf{w}_R \longrightarrow \mathbf{w}$$

we have consistency of the numerical source with the source term.

2.2.1 Roe's Q scheme

Roe's Q scheme [13] takes $\mathbf{Q}_{i+\frac{1}{2},j}$ and $\mathbf{Q}_{i,j+\frac{1}{2}}$ equal to the Roe averaged Jacobian matrices $\tilde{\mathbf{A}}$ and $\tilde{\mathbf{B}}$, i.e.

$$\mathbf{Q}^n_{i+\frac{1}{2},j} = \mathbf{Q}\left(\mathbf{w}^n_{i,j}, \mathbf{w}^n_{i+1,j}\right) = \tilde{\mathbf{A}} \quad \text{and} \quad \mathbf{Q}^n_{i,j+\frac{1}{2}} = \mathbf{Q}\left(\mathbf{w}^n_{i,j}, \mathbf{w}^n_{i,j+1}\right) = \tilde{\mathbf{B}}.$$

where

$$\tilde{\mathbf{A}} = \mathbf{A}\left(\tilde{\mathbf{w}}\right) \approx \frac{\partial \mathbf{F}}{\partial \mathbf{w}} \quad \text{and} \quad \tilde{\mathbf{B}} = \mathbf{B}\left(\tilde{\mathbf{w}}\right) \approx \frac{\partial \mathbf{G}}{\partial \mathbf{w}}$$

are locally linearised Jacobian matrices. The term $\tilde{\mathbf{w}}$ is known as the Roe average of $\mathbf{w}_L$ and $\mathbf{w}_R$, where $\mathbf{w}_L$, $\mathbf{w}_R$ represent adjacent piecewise constant states. $\tilde{\mathbf{A}}$, $\tilde{\mathbf{B}}$ and therefore $\mathbf{Q}$ are chosen so that the following properties are satisfied

- $\mathbf{Q}(\mathbf{w}_L, \mathbf{w}_R)$ is diagonalisable with real eigenvalues (hyperbolicity);
- $\mathbf{Q}(\mathbf{w}_L, \mathbf{w}_R) \longrightarrow \mathbf{Q}(\mathbf{w})$ as $\mathbf{w}_L, \mathbf{w}_R \longrightarrow \mathbf{w}$ (consistency);
- $\mathbf{F}(\mathbf{w}_{L,j}) - \mathbf{F}(\mathbf{w}_{R,j}) = \mathbf{Q}(\mathbf{w}_{L,j}, \mathbf{w}_{R,j})(\mathbf{w}_{L,j} - \mathbf{w}_{R,j})$ and;
- $\mathbf{G}(\mathbf{w}_{i,L}) - \mathbf{G}(\mathbf{w}_{i,R}) = \mathbf{Q}(\mathbf{w}_{i,L}, \mathbf{w}_{i,R})(\mathbf{w}_{i,L} - \mathbf{w}_{i,R})$ (conservation).

The final property ensures that we obtain a conservative algorithm and that any discontinuity moves at the correct speed.

By discretising the system (2.1) separately in the two coordinate directions we obtain expressions for $\tilde{\mathbf{w}}$ and $\mathbf{Q}$ along the x and y coordinate lines respectively. Equations (2.6) - (2.10) can then be used to give the two dimensional numerical flux and numerical source functions.

Chapter 3

The Shallow Water Equations

Meteorology and weather prediction are both fields in which conservation laws apply. The equations used to describe atmosphere and ocean processes are often too complex to solve analytically. In this case numerical methods are applied to obtain an approximate solution.

The shallow water equations can be used to simulate the flow of water in rivers, lakes and coastal regions. Thus they provide a valuable means for modelling a variety of problems related to the environment and coastal engineering etc. For instance, sediment transport in coastal regions has recently become a major topic of interest in the hydraulics industry [9].

3.1 The Equations

In this section we introduce the equations governing the flow of an incompressible fluid in a shallow domain, i.e. a domain whose depth is small relative to the dimensions of the problem. Initially, we will consider the shallow water approximation in the case of irrotational flow before introducing the effect

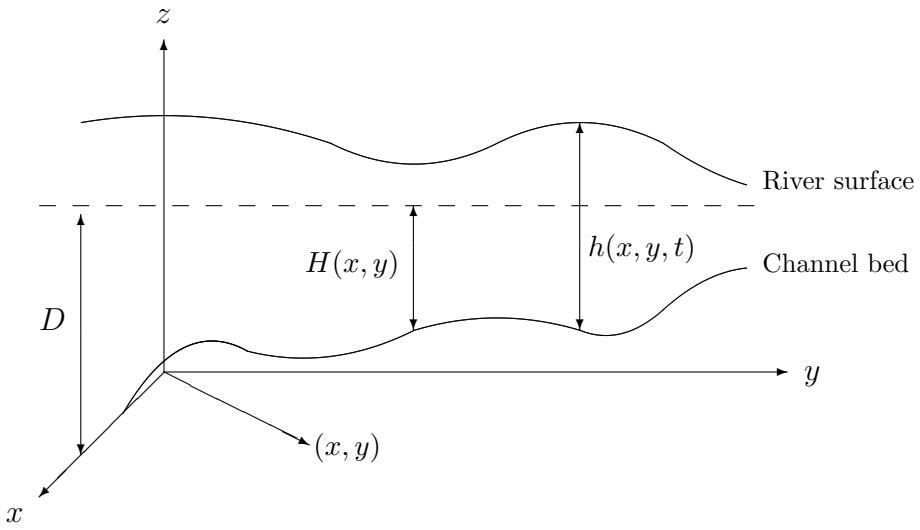

Figure 3.1: The shallow water domain

of the Earth's rotation in the form of a coriolis term. In two dimensions the shallow water equations comprise of the equation for conservation of mass

$$h_t + (uh)_x + (vh)_y = 0, \tag{3.1}$$

plus equations for conservation of momentum

$$u_t + uu_x + vu_y + gh_x = gH_x, \tag{3.2}$$

$$v_t + uv_x + vv_y + gh_y = gH_y. \tag{3.3}$$

The function $h(x, y, t)$ represents the height of the fluid above the bottom of the channel at the point (x, y) at a time t, $u(x, y, t)$ and $v(x, y, t)$ are the fluid velocity in the x and y directions respectively, $H(x, y, t)$ is the depth

of the fluid at the same point but from a fixed reference level, and g is the gravitational constant, see figure 3.1. It is often convenient to rewrite $H(x, y)$ in terms of the bed height $B(x, y)$

$$H(x, y) = D - B(x, y).$$

3.2 Conservation form

To rewrite the system (3.1) - (3.3) in generalised conservation form we first multiply (3.1) by u,

$$uh_t + u(uh)_x + u(hv)_y = 0. \tag{3.4}$$

Using the product rule

$$(uh)_t = hu_t + uh_t,$$

to substitute in for hu_t after multiplying (3.2) by h gives

$$(uh)_t - uh_t + (hu)u_x + (hv)u_y + ghh_x = ghH_x. \tag{3.5}$$

Using (3.4) and the product rule on $(hu^2)_x$, $(huv)_y$ and $(gh^2)_x$, i.e.

$$\begin{aligned} (huu)_x &= (hu)_x u + (hu)u_x \\ (huv)_y &= (hv)_y u + (hv)u_y \\ (gh^2)_x &= 2ghh_x \end{aligned}$$

and substituting into (3.5) we obtain (3.2) with the left hand side in conservative form

$$(uh)_t + (u^2 h + \frac{1}{2}gh^2)_x + (huv)_y = ghH_x.$$

Following a similar procedure for (3.3) yields

$$(vh)_t + (huv)_x + (v^2 h + \frac{1}{2}gh^2)_y = ghH_y.$$

We can now write the system in vector form as

$$\begin{bmatrix} h \\ uh \\ vh \end{bmatrix}_t + \begin{bmatrix} uh \\ hu^2 + \frac{1}{2}gh^2 \\ huv \end{bmatrix}_x + \begin{bmatrix} vh \\ huv \\ hv^2 + \frac{1}{2}gh^2 \end{bmatrix}_y = \begin{bmatrix} 0 \\ ghH_x \\ ghH_y \end{bmatrix}. \qquad (3.6)$$

The nonlinear character of the shallow water equations means that analytical solutions are limited to only a few special cases (see Thacker [17]). Over the past twenty years many papers have looked at using finite element and finite difference methods to solve these equations numerically, for example, see Glaister [4]. In [8] Hudson tests a variety of numerical techniques for approximating the one dimensional shallow water equations by using a series of test problems in which the source term $\mathbf{R}$ becomes more significant, i.e. the variation of the riverbed becomes more pronounced. In [9] he considers the extension of some of these techniques to the two dimensional case, using a 2D wave propagation test problem to determine which of the schemes is the most accurate.

In [2] Bermúdez & Vázquez focus on the application of the methods introduced in [1] (see section 2.2) to the variable depth shallow water equations. The performance of the schemes is compared in terms of a *C-property* introduced to prevent spurious numerical waves. In the next section we explain the significance of this C-property in terms of the behaviour of the numerical scheme.

3.3 C-Property

Bermúdez & Vázquez [1] introduce the C-property as a requirement for the good behaviour of a numerical scheme. Consider the 2D shallow water equations for the quiescent flow case,

$$u(x,y,t) \equiv 0, \quad v(x,y,t) \equiv 0 \quad \text{and} \quad h(x,y,t) \equiv H \quad \text{for all } (x,y,t).$$

In the stationary case $\mathbf{w}_t = 0$ and thus the system (3.6) reduces to

$$\mathbf{F}(\mathbf{w})_x + \mathbf{G}(\mathbf{w})_y = \mathbf{R}. \tag{3.7}$$

By rewriting the source term as

$$\mathbf{R} = \mathbf{f} + \mathbf{g}$$

we can split (3.7) in two separate equations

$$\mathbf{F}(\mathbf{w})_x = \mathbf{f} \quad \text{and} \quad \mathbf{G}(\mathbf{w})_y = \mathbf{g} \tag{3.8}$$

so that the flux and source terms balance. To ensure that a numerical scheme is accurate and well behaved, both sides of equations (3.8) should be discretised in a similar way, i.e. the numerical fluxes and numerical source terms should also balance,

$$\mathbf{F}^*_{i+\frac{1}{2},j} - \mathbf{F}^*_{i-\frac{1}{2},j} = \mathbf{f}^*_{i,j} \quad \text{and} \quad \mathbf{G}^*_{i,j+\frac{1}{2}} - \mathbf{G}^*_{i,j-\frac{1}{2}} = \mathbf{g}^*_{i,j}.$$

If the source term approximations balance with the numerical fluxes then the numerical scheme is said to satisfy:

- the approximate C-property if it is accurate to the order $O(\Delta x^2)$ when applied to the quiescent flow case;

- the exact C-property, if it is exact when applied to the quiescent flow case.

If the C-property is not satisfied parasitic waves may appear in the numerical solution.

3.4 Test problem A

We wish to consider the propagation of a wave in an enclosed rectangular region $D = \{(x, y) : x_0 \leq x \leq x_M, y_0 \leq y \leq y_N\}$.

For this problem the riverbed is defined as

$$B(x,y) = \begin{cases} 0.5\left(\cos^2\left(\frac{(x-0.5)\pi}{0.25}\right)\cos^2\left(\frac{(y-0.5)\pi}{0.25}\right)\right) & \text{if} \quad 0.375 < x < 0.625, \\ & \text{and } 0.375 < y < 0.625 \\ 0 & \text{otherwise} \end{cases}$$

which represents a mound positioned in the centre of the region as is illustrated in figure 3.2.

We have the initial conditions

$$h(x,y,0) = \begin{cases} 1 + 0.25\left(\cos^2\left(\frac{(x-0.225)\pi}{0.25}\right)\cos^2\left(\frac{(y-0.5)\pi}{0.25}\right)\right) & \text{if} \quad 0.1 < x < 0.35, \\ & \text{and } 0.375 < y < 0.625 \\ 1 - B(x,y) & \text{otherwise} \end{cases}$$

$$u(x,y,0) = 0, \quad v(x,y,0) = 0.$$

Boundary conditions are required at the upstream and downstream boundaries and along the sides of the channel. Since walls are present at all boundaries

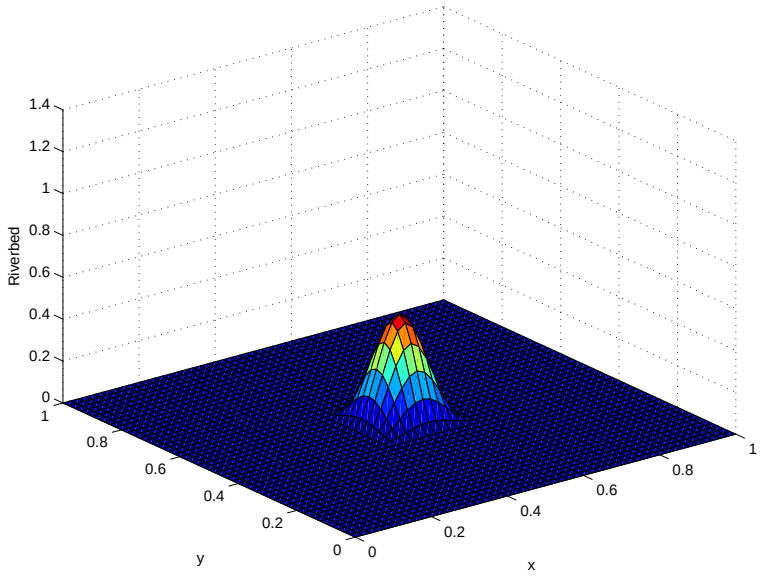

Figure 3.2: The riverbed

we need to reflect the velocity

$$u^n_{-1,j} = -u^n_{0,j}, \quad u^n_{M+1,j} = -u^n_{M,j}, \quad v^n_{i,-1} = -v^n_{i,0}, \quad \text{and} \quad v^n_{i,N+1} = -v^n_{i,N}.$$

This means that the flow in the direction of the outward normal does not cross the boundary - instead it is reflected back into the region. The flow tangential to the boundary remains the same. We will assume that the water depth is constant at the boundaries, giving the simple conditions

$$h^n_{-1,j} = h^n_{0,j}, \quad h^n_{M+1,j} = h^n_{M,j}, \quad h^n_{i,-1} = h^n_{i,0} \quad \text{and} \quad h^n_{i,N+1} = h^n_{i,N}.$$

3.5 Roe's Q Scheme

To apply Roe's Q scheme we require an approximation of the Jacobian matrices $\tilde{\mathbf{A}}$ and $\tilde{\mathbf{B}}$. In [4] Glaister determines the following Roe averaged

Jacobian matrices for the 2D shallow water equations,

$$\tilde{\mathbf{A}} = \frac{\partial \mathbf{F}}{\partial \mathbf{w}} = \begin{bmatrix} 0 & 1 & 0 \\ \tilde{c}^2 - \tilde{u}^2 & 2\tilde{u} & 0 \\ -\tilde{u}\tilde{v} & \tilde{v} & \tilde{u} \end{bmatrix} \quad \text{and} \quad \tilde{\mathbf{B}} = \frac{\partial \mathbf{G}}{\partial \mathbf{w}} = \begin{bmatrix} 0 & 0 & 1 \\ -\tilde{u}\tilde{v} & \tilde{v} & \tilde{u} \\ \tilde{c}^2 - \tilde{u}^2 & 0 & 2\tilde{v} \end{bmatrix},$$

where $\tilde{c} = \sqrt{g\tilde{h}}$ is the wave speed.

The corresponding eigenvalues and eigenvectors for $\tilde{\mathbf{A}}$ are

$$\tilde{\lambda}_1^F = \tilde{u} - \tilde{c}, \quad \tilde{\lambda}_2^F = \tilde{u}, \quad \tilde{\lambda}_3^F = \tilde{u} + \tilde{c},$$

and

$$\tilde{\mathbf{e}}_1^F = \begin{bmatrix} 1 \\ \tilde{u} - \tilde{c} \\ \tilde{v} \end{bmatrix}, \quad \tilde{\mathbf{e}}_2^F = \begin{bmatrix} 0 \\ 0 \\ 1 \end{bmatrix}, \quad \tilde{\mathbf{e}}_3^F = \begin{bmatrix} 1 \\ \tilde{u} + \tilde{c} \\ \tilde{v} \end{bmatrix}.$$

Whilst for matrix $\tilde{\mathbf{B}}$ we have

$$\tilde{\lambda}_1^G = \tilde{v} - \tilde{c}, \quad \tilde{\lambda}_2^G = \tilde{v}, \quad \tilde{\lambda}_3^G = \tilde{v} + \tilde{c},$$

and

$$\tilde{\mathbf{e}}_1^G = \begin{bmatrix} 1 \\ \tilde{u} \\ \tilde{v} - \tilde{c} \end{bmatrix}, \quad \tilde{\mathbf{e}}_2^G = \begin{bmatrix} 0 \\ 1 \\ 0 \end{bmatrix}, \quad \tilde{\mathbf{e}}_3^G = \begin{bmatrix} 1 \\ \tilde{u} \\ \tilde{v} + \tilde{c} \end{bmatrix}.$$

The Roe averages are given by

$$\tilde{u} = \frac{\sqrt{h_R}u_R + \sqrt{h_L}u_L}{\sqrt{h_R} + \sqrt{h_L}}, \quad \tilde{v} = \frac{\sqrt{h_R}v_R + \sqrt{h_L}v_L}{\sqrt{h_R} + \sqrt{h_L}} \quad \text{and} \quad \tilde{h} = \frac{1}{2}(h_R + h_L),$$

where the subscripts L and R denote two adjacent states (left and right) at points L and R on either the x or y coordinate line. These averages are not unique, however by choosing $\tilde{h}$ equal to the arithmetic mean of h_L and h_R and taking

$$\hat{\mathbf{f}}^n_{i+\frac{1}{2},j} = \begin{bmatrix} 0 \\ g\left(\frac{h^n_{i,j}+h^n_{i+1,j}}{2}\right)\left(\frac{H_{i+1,j}-H_{i,j}}{\Delta x}\right) \\ 0 \end{bmatrix},$$

and

$$\hat{\mathbf{g}}^n_{i,j+\frac{1}{2}} = \begin{bmatrix} 0 \\ 0 \\ g\left(\frac{h^n_{i,j}+h^n_{i,j+1}}{2}\right)\left(\frac{H_{i,j+1}-H_{i,j}}{\Delta y}\right) \end{bmatrix}$$

for the source term approximation, we ensure that the C-property discussed in section 3.3 is exactly satisfied.

We are now in a position to apply Roe's Q scheme to test problem A.

3.6 Rotation

We can incorporate the effect of the Earth's rotation into the shallow water equations by including an additional term $\mathbf{s}$ on the right hand side of (3.6) where

$$\mathbf{s} = \begin{bmatrix} 0 \\ fvh \\ -fuh \end{bmatrix}.$$

The Coriolis parameter, f, is given by $f = 2\Omega \sin\phi$ where $\Omega = 7.292\times10^{-5}s^{-1}$ is the rotation rate of the earth and ϕ is latitude. The source term is then given by

$$\mathbf{R} = \mathbf{f} + \mathbf{g} = \begin{bmatrix} 0 \\ fvh + ghH_x \\ 0 \end{bmatrix} + \begin{bmatrix} 0 \\ 0 \\ -fuh + ghH_y \end{bmatrix}.$$

For the source term approximations $\hat{\mathbf{f}}$ and $\hat{\mathbf{g}}$ we use the Roe average values $\tilde{u}$ and $\tilde{v}$.

3.6.1 The β-plane approximation

The use of local cartesian coordinates and the restriction of our attention to only a small region of the globe allows us to model the Earth's surface as a plane, thus avoiding the complications of spherical geometry. However, we can retain the leading order effect of the Earth's curvature by taking into account the variation of the coriolis parameter, f, with latitude.

The β plane approximation, introduced by C.G Rossby [14], assumes that f varies linearly with the meridional (North-South) distance y. If we let ϕ_0 be the latitude at the origin of our cartesian coordinates, and expand f in a Taylor series about ϕ_0 we get,

$$f(\phi_0 + \delta\phi) = f(\phi_0) + \delta\phi f'(\phi_0) + O(\delta\phi^2),$$

for small $\delta\phi$, $y = a\delta\phi$, so that

$$\begin{aligned} f &= 2\Omega\sin\phi_0 + \frac{2\Omega\cos\phi_0}{a}y \\ &= f_0 + \beta y, \end{aligned}$$

where $a = 6.37 \times 10^6$ is the mean radius of the Earth, and $\beta = \frac{df}{dy} = \frac{2\Omega \cos \phi_0}{a}$. If the origin of our coordinate system lies on the equator, then $\phi_0 = 0$, $f_0 = 0$ and

$$f = \frac{2\Omega}{a} y = \beta y.$$

3.6.2 Inertial Motion

The coriolis "force"

$$\mathbf{F}_c = -2\boldsymbol{\Omega} \times \mathbf{u}$$

acts at right angles to the velocity $\mathbf{u}$ (and also to $\boldsymbol{\Omega}$) and hence cannot change the speed of a fluid particle. However, it will change the direction of motion.

Consider an open mass of water, such as the ocean. The water is set in motion by an initial impulse, such as a local wind blowing across its surface. It then moves under the influence of the coriolis force and gravity. If there are no other forces acting on the water the movement of the current will be circular.

Now consider a particle moving around a circle of radius R on a plane rotating with angular velocity Ω about the origin. Since the particle travels a distance of $2\pi R$ in time $2\pi/\Omega$, its speed of motion U is given by

$$U = \frac{2\pi R}{2\pi/\Omega} = \Omega R. \tag{3.9}$$

When Ω and R are known, we can use the relationship (3.9) to find the horizontal velocity components u and v. We can specify the curve

$$U^2 = u^2 + v^2,$$

by the pair of parametric equations,

$$u = U \sin ft \tag{3.10}$$

$$v = U \cos ft, \tag{3.11}$$

thus giving u and v as functions of time and the Earth's rotation. Such motion is called *inertial motion* or *inertial oscillation*.

3.7 Test Problem B

In this problem we wish to simulate the inertial currents observed on the ocean's surface. The domain is a rotating plane, and for simplicity we will assume that the origin of our coordinate system is on the axis of rotation. The seabed is taken to be flat, giving an initially undisturbed surface,

$$h(x, y, 0) = constant,$$

with zero initial velocity

$$u(x, y, 0) = 0, \quad \text{and} \quad v(x, y, 0) = 0.$$

The boundaries are prescribed velocities of the form 3.10 and 3.11.

3.8 Numerical Results

3.8.1 Test Problem A

Figures 3.3 show the results of Roe's Q scheme applied to test problem A. The scheme was used with step-sizes $\Delta x = \Delta y = 0.02$, and$\Delta t = 0.002$. For this problem the variable riverbed is given by a cosine squared bell

positioned in the centre of the channel. The initial conditions represent an initial pulse on the water's surface which rapidly loses height as it splits and propagates outward in all directions. One of these waves passes over the hump in the riverbed becoming partially reflected. The left moving waves hit the boundary at $x = 0$ and are split further. Since walls are present reflection occurs.

Results are only shown up to a final time of $t = 0.8$, beyond which the waves continue to disperse, rebounding back into the region as they hit the sides of the channel. The surface of the water begins to flatten as the waves gradually become smaller and smaller in amplitude.

It is difficult to evaluate the performance of Roe's Q scheme since no analytical solutions are available for comparison. The results are smooth and appear to be free from any spurious oscillations. However, Roe's scheme is only first order and therefore dissipative. Dissipation occurs when the amplitude of the travelling waves are damped resulting in the numerical solution being smeared. Hence the apparent flattening of the water surface.

3.8.2 Test Problem B

Figures 3.4 show the surface elevation $(h + B)$ for a 100 km$\times$100 km region of water, with spatial step sizes $\Delta x = \Delta y = 2$ km and a time step of 0.1 seconds. Initially the water surface is undisturbed. An impulse is generated at the edge of the domain by the boundary conditions, thus setting the water in motion. The mass of water then continues to move due to its inertia.

As with test problem A, the results obtained from Roe's Q Scheme are smooth and do not exhibit any parasitic waves. Yet again the scheme is

very diffusive. After an initial increase, the amplitude of the waves rapidly become damped. We can reduce this problem to some extent by decreasing the spatial step size (compare figures 3.5). However, in practice the extent of this improvement has to be weighed against the increased running time of the code.

A more practical way of minimising this dissipation is to use a numerical method which satisfies the Total Variation Diminishing (TVD) property. Such schemes are known as high-resolution schemes (for more detail see [18]). One approach that can be used to derive a high resolution, second order, oscillation free scheme is that of Flux limiter methods. These add a limited anti-diffusive flux to the first order scheme. This flux is limited using a flux limiter Φ to ensure that the scheme is TVD. Φ is chosen such that if the data is smooth, it's value is 1, thus reverting the numerical flux to a second order approximation, but if the data is near a discontinuity, $\Phi = 0$ which reverts the numerical flux to a first order approximation. In [16] Sweby presents a class of limiters that guarantee second order accuracy whilst still retaining the TVD property.

Figures 3.6 and 3.7 show the effect of introducing a gently sloping riverbed into problem B,

$$B(x, y) = 1.0 - 0.01y.$$

The depth function is now given by

$$h(x, y, 0) = 2.0 - B(x, y)$$

and is illustrated in the first of figures 3.6. Comparing figures 3.6 and 3.7 with figures 3.4 we observe that the flow has become orientated in the direction of the sloping bed. The waves are greater in amplitude than for the flat bed

case, and their periodic motion is more clearly visible. The initial height of the surface is not maintained and decreases as time increases. At times $t = 90$ & $t = 180$, and $t = 120$ & $t = 240$ (figures 3.7) the wave profiles are almost identical, but the scales to the side of each plot show that the surface height has actually dropped. Again this could be due to the diffusive nature of Roe's scheme.

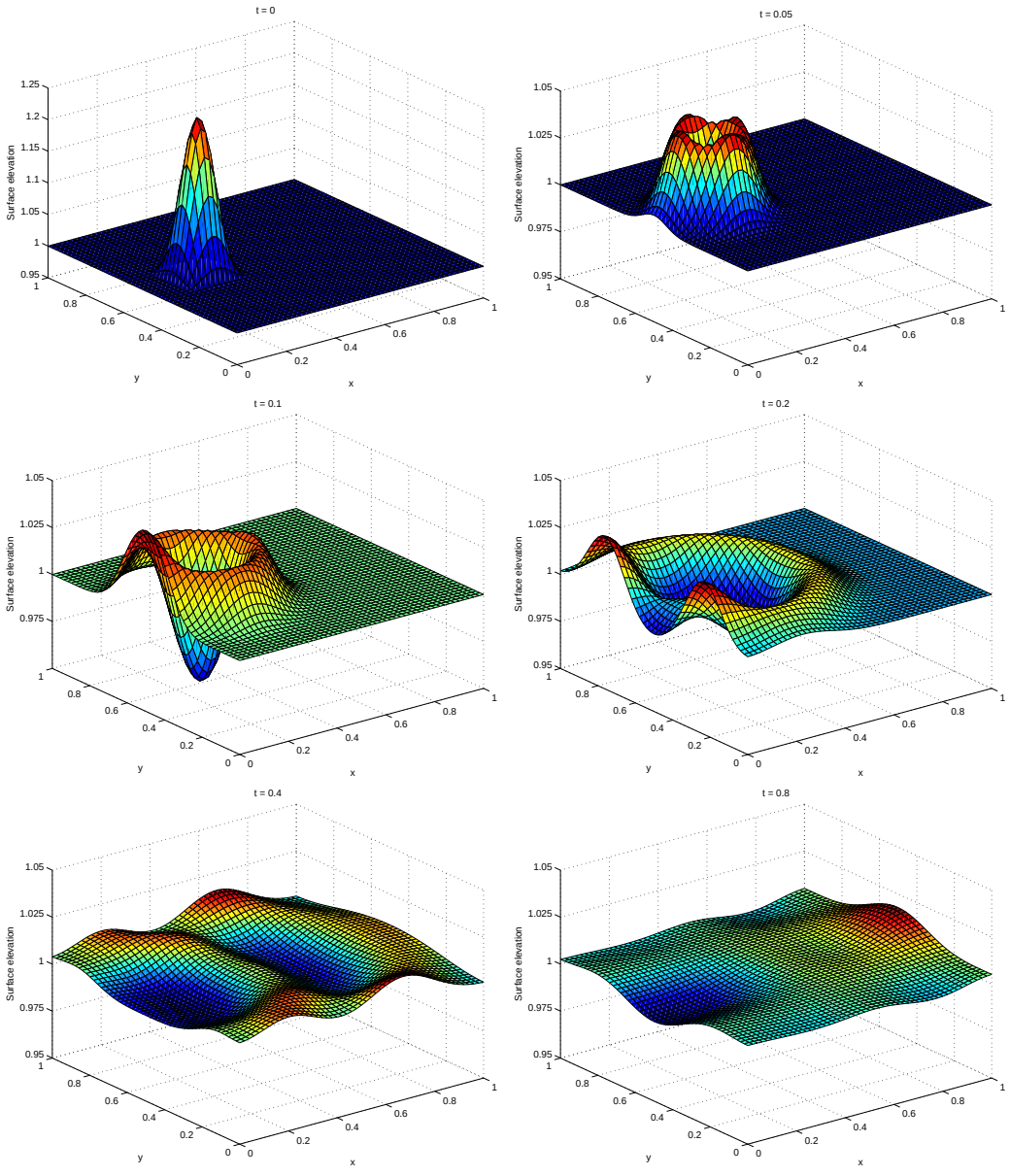

Figure 3.3: Numerical results of Roe's Q Scheme for test problem A - Surface elevation $(h + B)$.

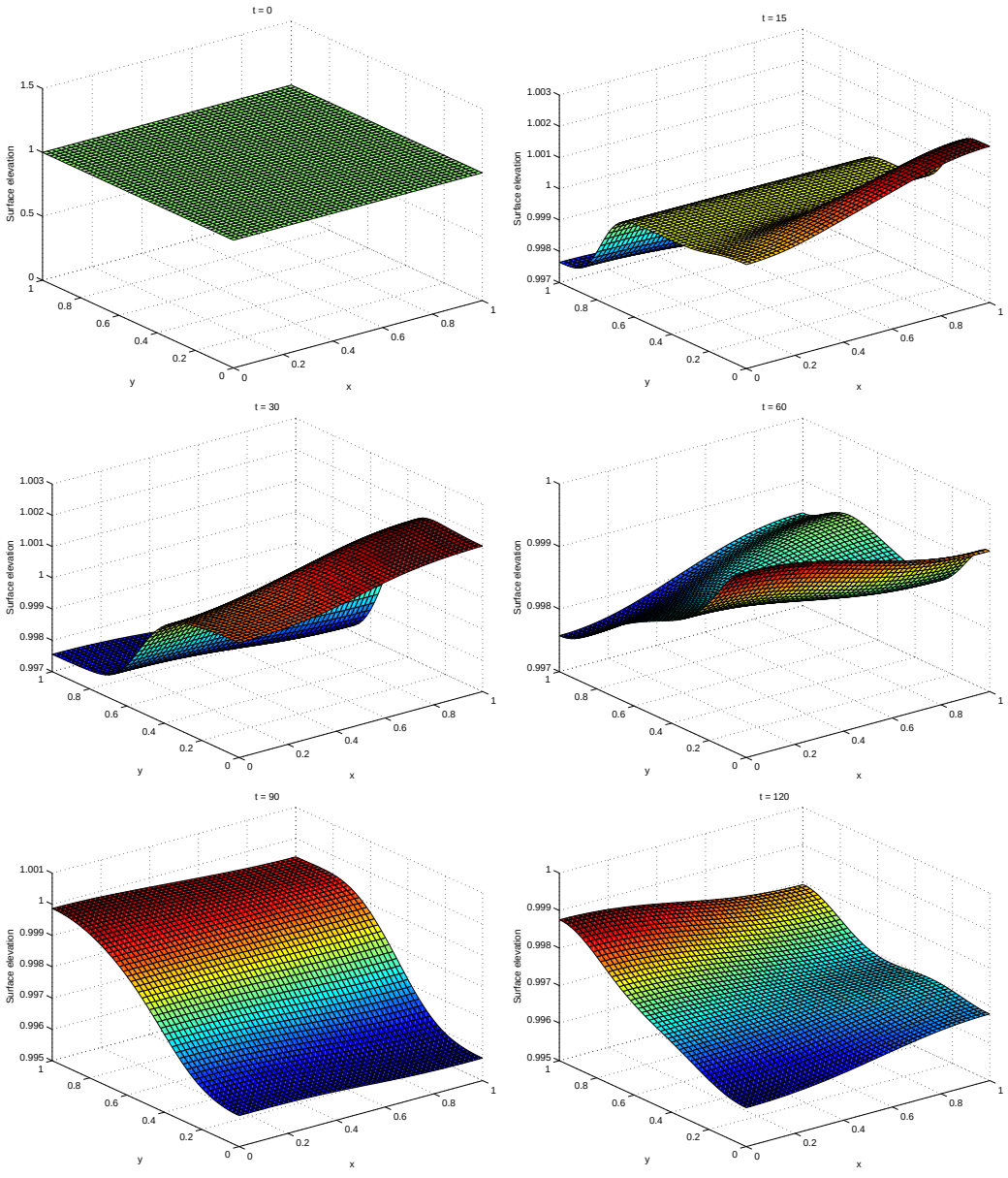

Figure 3.4: Numerical results of Roe's Q Scheme for test problem B - Surface elevation $(h + B)$.

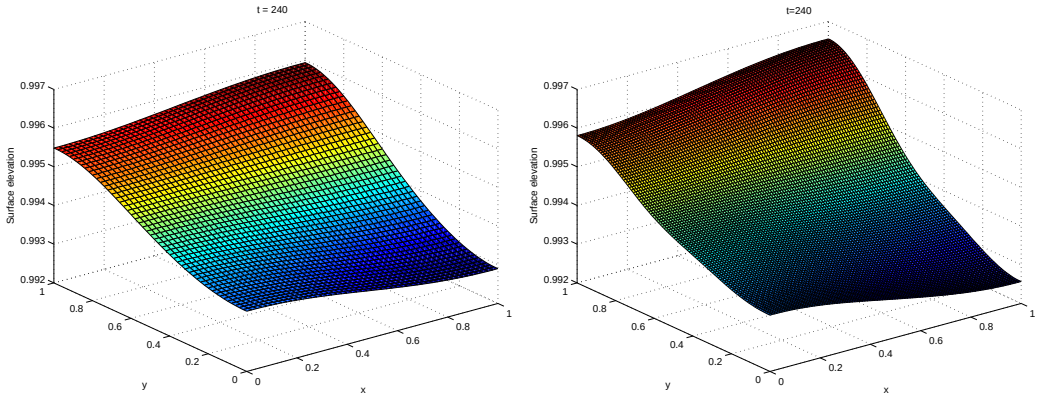

Figure 3.5: Illustration of the effect of halving the spatial step size from $\Delta x = \Delta y = 2$ to $\Delta x = \Delta y = 1$.

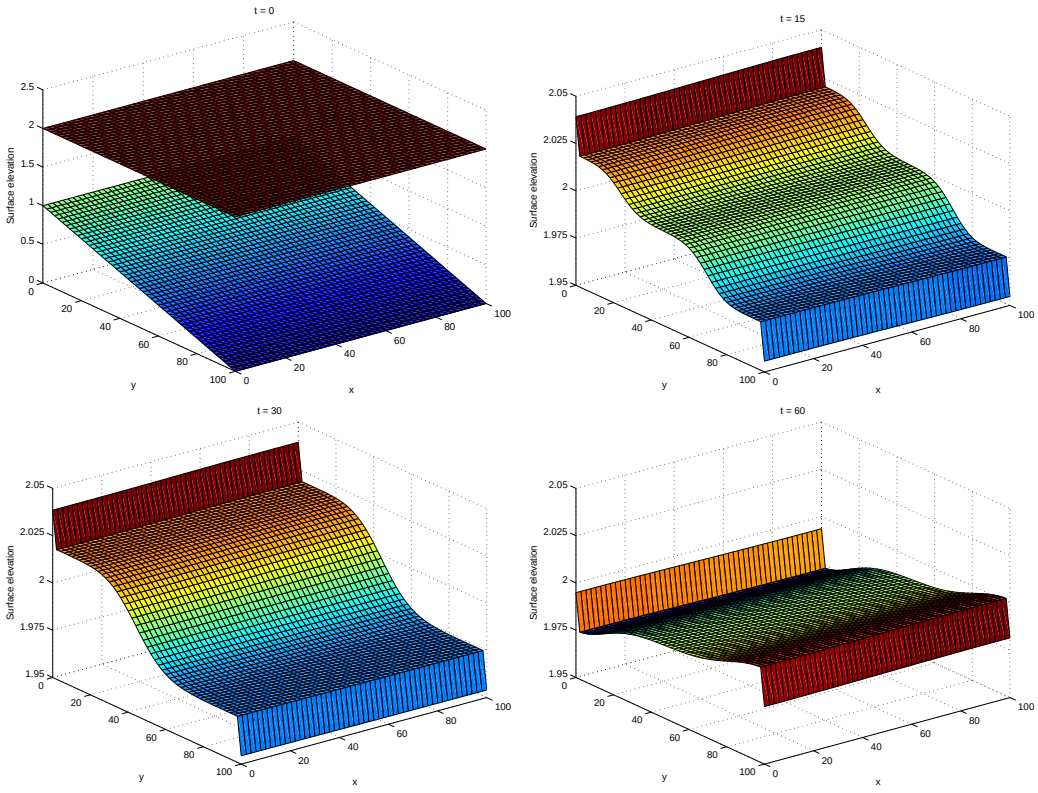

Figure 3.6: Numerical results of Roe's Q Scheme for test problem B with variable riverbed - Surface elevation $(h + B)$.

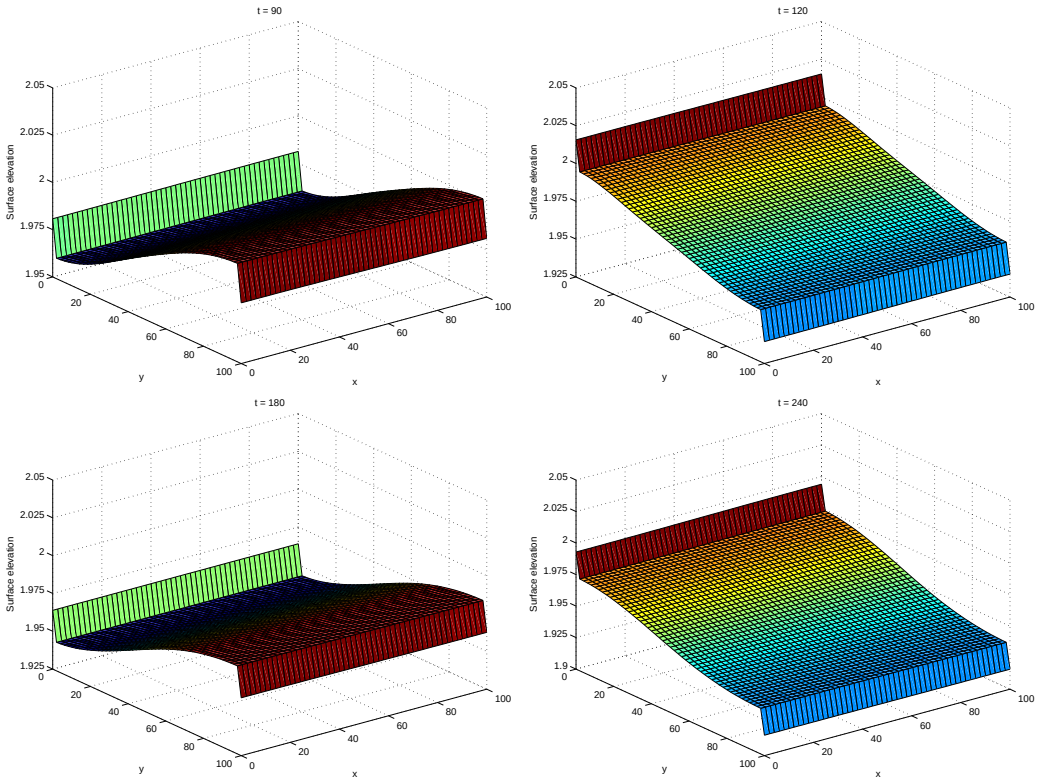

Figure 3.7: Numerical results of Roe's Q Scheme for test problem B with variable riverbed - Surface elevation $(h + B)$.

Chapter 4

Crowd Dynamics

4.1 Introduction

The movement of people within crowds is a complex phenomenon that has been studied for over 40 years. It is of interest in numerous fields such as building development, event management and, particularly in more recent years, emergency planning for evacuation and disaster. Pedestrian movement shares a number of characteristics with traffic flow. Models initially developed to describe traffic flow have successfully been adapted and applied to crowds. Much of the work so far has focused on modelling in one dimension, since traffic naturally moves in single lane formation. Pedestrians, however, tend to inhabit domains where movement is less restricted and can be multi-directional. The aim of this study is to extend the one dimensional model proposed by Payne and Whitham [19] and consider a more realistic two dimensional situation in which individuals can overtake each other and, for example, move across a room towards a doorway.

There are two main approaches to modelling crowds; *microscopic* and *macroscopic*. Microscopic models consider the individual preferences of each pedestrian and look to capture more of the psychological aspects of human behaviour. They consider how individual pedestrians react to their surroundings, adjusting their behaviour based on the conditions ahead. Dirk Helbing has published many papers in this area (see *www.helbing.org* for more details). An alternative approach is to consider the overall average behaviour of the crowd as a whole by treating the crowd as a single body with continuous velocity and density fields. This continuum type model is referred to as Macroscopic. Although microscopic models are considered more advantageous in terms of capturing individual sensitivities and interaction behaviour they involve the resolution of a large number of individual parameters and are therefore very expensive. Conversely, macroscopic models are much easier to apply and are generally more computationally efficient. The work of this study will be based on a Macroscopic model proposed by Payne and Whitham [19].

4.2 The Payne Whitham model

The Payne Whitham model was developed in the 1970's and was initially inspired by the similarities between traffic flow and fluid dynamics. Here we adapt it for crowd flow.

In two dimensions the model consists of the continuity equation

$$\rho_t + (\rho u)_x + (\rho v)_y = 0, \tag{4.1}$$

where $\rho(x, y, t)$ is the density and $u(x, y, t)$, $v(x, y, t)$ are the velocities (ms^{-1})

in the x and y directions respectively, combined with two dynamic equations derived from the Navier Stokes equations of motion for a compressible fluid, but with a pressure $p = C_0^2\rho$ and with the addition of a relaxation term, thus giving

$$u_t + uu_x + vu_y = \frac{U(\rho) - u}{\tau} - \frac{C(\rho)}{\rho}\rho_x \tag{4.2}$$

$$v_t + uv_x + vv_y = \frac{V(\rho) - v}{\tau} - \frac{C(\rho)}{\rho}\rho_y, \tag{4.3}$$

where τ is the relaxation time and $U(\rho)$, $V(\rho)$ are functions representing the desired velocity of a pedestrian for a given crowd density. $C(\rho)$ is the anticipation coefficient, which here we take to be $C(\rho) = C_0^2$ where C_0 is a constant. For a more detailed discussion on this see [12] & [21].

The relaxation term describes interactions between pedestrians and aims to capture the way in which individuals adjust their velocity towards an optimal value, given by the velocity function. If an individual's speed is greater than this value then the relaxation term has the effect of slowing the pedestrian down. Conversely, if the individual is moving at a speed less than the desired value the relaxation term speeds the individual up. This change is not instantaneous, the average time required for this process being given by the relaxation time τ.

This is a much studied model and several variations to it have been suggested. The model has been criticised as under certain conditions it allows negative wave speeds, thus enabling individuals to travel backwards against the fluid flow. In addition, the wave propagation speeds (given by the eigenvalues of the Jacobian matrices of the system 4.4) are such that one will always be greater than the velocity of the fluid flow. This implies that infor-

mation can travel faster than the flow and reach fluid particles from behind. In terms of traffic modelling, the isotropic nature of the Payne Whitham model contradicts the generally held belief that traffic is an anisotropic fluid. Drivers on a single lane motorway will mainly react to conditions on the road ahead of their vehicle. Although the characteristics of pedestrian interaction are also primarily anisotropic there will be some influence from those behind, particularly in crowds where individuals are moving in close proximity to one another. This model limits us to those interactions that are isotropic assuming that the crowd responds equally to information from behind as well as from in front.

4.2.1 Conservation form

Proceeding in a similar manner to section 3.2 we can rewrite (4.1), (4.2) and (4.3) in the conservative vector form

$$\begin{bmatrix} \rho \\ \rho u \\ \rho v \end{bmatrix}_t + \begin{bmatrix} \rho u \\ \rho u^2 + C_0^2 \rho \\ \rho uv \end{bmatrix}_x + \begin{bmatrix} \rho v \\ \rho uv \\ \rho v^2 + c_0^2 \rho \end{bmatrix}_y = \begin{bmatrix} 0 \\ \rho \frac{(U(\rho)-u)}{\tau} \\ \rho \frac{(V(\rho)-v)}{\tau} \end{bmatrix}. \qquad (4.4)$$

4.3 Roe's Q Scheme

The Roe averaged Jacobian matrices of the fluxes are given by

$$\tilde{\mathbf{A}} = \frac{\partial \mathbf{F}}{\partial \mathbf{u}} = \begin{bmatrix} 0 & 1 & 0 \\ C_0^2 - \tilde{u}^2 & 2\tilde{u} & 0 \\ -\tilde{u}\tilde{v} & \tilde{v} & \tilde{u} \end{bmatrix} \quad \text{and} \quad \mathbf{B} = \frac{\partial \mathbf{G}}{\partial \mathbf{u}} = \begin{bmatrix} 0 & 0 & 1 \\ -\tilde{u}\tilde{v} & \tilde{v} & \tilde{u} \\ C_0^2 - \tilde{u}^2 & 0 & 2\tilde{v} \end{bmatrix},$$

The corresponding eigenvalues and eigenvectors for $\tilde{\mathbf{A}}$ are

$$\tilde{\lambda}_1^F = \tilde{u} - C_0, \quad \tilde{\lambda}_2^F = \tilde{u}, \quad \tilde{\lambda}_3^F = \tilde{u} + C_0,$$

and

$$\tilde{\mathbf{e}}_1^F = \begin{bmatrix} 1 \\ \tilde{u} - C_0 \\ \tilde{v} \end{bmatrix}, \quad \tilde{\mathbf{e}}_2^F = \begin{bmatrix} 0 \\ 0 \\ C_0 \end{bmatrix}, \quad \tilde{\mathbf{e}}_3^F = \begin{bmatrix} 1 \\ \tilde{u} + C_0 \\ \tilde{v} \end{bmatrix}.$$

For matrix $\tilde{\mathbf{B}}$ we have

$$\tilde{\lambda}_1^G = \tilde{v} - C_0, \quad \tilde{\lambda}_2^G = \tilde{v}, \quad \tilde{\lambda}_3^G = \tilde{v} + C_0,$$

and

$$\tilde{\mathbf{e}}_1^G = \begin{bmatrix} 1 \\ \tilde{u} \\ \tilde{v} - C_0 \end{bmatrix}, \quad \tilde{\mathbf{e}}_2^G = \begin{bmatrix} 0 \\ -C_0 \\ 0 \end{bmatrix}, \quad \tilde{\mathbf{e}}_3^G = \begin{bmatrix} 1 \\ \tilde{u} \\ \tilde{v} + C_0 \end{bmatrix}.$$

The Roe averages are given by

$$\tilde{u} = \frac{\sqrt{\rho_R}u_R + \sqrt{\rho_L}u_L}{\sqrt{\rho_R} + \sqrt{\rho_L}}, \quad \tilde{v} = \frac{\sqrt{\rho_R}v_R + \sqrt{\rho_L}v_L}{\sqrt{\rho_R} + \sqrt{\rho_L}} \quad \text{and} \quad \tilde{\rho} = \sqrt{\rho_R \rho_L}.$$

4.4 The Velocity Function

The exact form of the velocity function is dependent on the nature of the physical situation and as a consequence many choices have been proposed, see [12]. A pedestrians movement is guided by his or her desired velocity which is composed of a desired speed and a desired direction. It is assumed that desired speed has mean $1.34ms^{-1}$ and standard deviation $0.26ms^{-1}$

[10]. The desired direction of movement is given by the pedestrian's intended destination.

4.4.1 The Bee-line Effect

In this report we consider the bee-line effect where pedestrians wish to move towards a specific target, such as an exit, positioned at certain point in the room. The pedestrians aim is to reach the point by taking the most direct route. We assume that movement is independent of density. If an individual at the point (x_i, y_j) wants to arrive at a destination (x_d, y_d) then their intended direction of movement is given by the unit vector

$$\hat{\mathbf{e}}_{i,j} = \frac{\mathbf{e}_{i,j}}{\|\mathbf{e}_{i,j}\|}$$

where

$$\mathbf{e}_{i,j} = \begin{bmatrix} (x_d - x_i) \\ (y_d - y_j) \end{bmatrix},$$

is the direction of travel, and

$$\|\mathbf{e}_{i,j}\| = \sqrt{(x_d - x_i)^2 + (y_d - y_j)^2}$$

is the remaining distance.

The velocity function $\mathbf{V} = U\mathbf{i} + V\mathbf{j}$ is then given by

$$\mathbf{V}_{i,j} = v^0_{i,j}\hat{\mathbf{e}}_{i,j},$$

where $v^0_{i,j}$ is the desired speed.

4.5 Initial and Boundary Conditions

To simulate the bee-line effect we need to first specify the initial and boundary conditions. We wish to consider a crowd in a rectangular room with solid walls. There is an exit along the wall $x = x_M$ towards which the crowd wishes to head. The initial conditions are given by a gaussian distribution of the form

$$\rho(x, y, 0) = \rho_0 \exp\left(-\frac{(x-a)^2}{c^2} - \frac{(y-b)^2}{d^2}\right),$$

and the crowd is initially at rest, i.e.

$$u(x, y, 0) = 0, \quad \text{and} \quad v(x, y, 0) = 0.$$

The question remains as to what to do at the boundaries. The solid walls of the room can be reproduced by imposing the slip boundary condition

$$\mathbf{u} \cdot \mathbf{n} = 0,$$

i.e. the pedestrians cannot walk through the walls but can move tangentially to them.

Equivalently we could use ghost points to obtain the reflective conditions

$$u^n_{-1,j} = -u^n_{0,j}, \quad u^n_{M+1,j} = -u^n_{M,j}, \quad v^n_{i,-1} = -v^n_{i,0}, \quad \text{and} \quad v^n_{i,N+1} = -v^n_{i,N}.$$

We need to prescribe conditions at the exit that will allow the pedestrians to pass out of the room. We could use the simple free flow condition

$$\mathbf{u}^n_{M+1,j} = \mathbf{u}^n_{M,j}.$$

However, we need to ensure that pedestrians do not re-enter the room via the exit. If the incorrect boundary conditions are used then the pedestrians may be reflected back into the domain resulting in an inaccurate numerical solution. Transmissive boundary conditions can be used to eliminate the left moving waves (pedestrians) but allow the right moving waves to pass through the boundary, thus enabling the crowd to leave the room without being reflected back. One type of transmissive boundary condition discussed by Godlewski and Raviart [5] can be obtained by using the k-Riemann invariants, given by

$$\frac{\partial r_k}{\partial \mathbf{u}} \cdot \mathbf{e}_k^F = 0 \tag{4.5}$$

and

$$\frac{\partial s_k}{\partial \mathbf{u}} \cdot \mathbf{e}_k^G = 0, \tag{4.6}$$

for the x and y sweeps respectively. $\mathbf{e}_k^F$ and $\mathbf{e}_k^G$ are the eigenvectors of the Jacobian matrices $\mathbf{A}$ and $\mathbf{B}$, and the r_k, s_k denote the k-Riemann invariants where k is the k^{th} component of the system. For the system (4.4) we have $k = 3$.

Since the exit lies along the boundary at $x = x_M$, we are only concerned with the direction of the u component of the pedestrians velocity and therefore need only consider solutions to (4.5), i.e.

$$\begin{aligned}
\frac{\partial r_1}{\partial \rho} + (u - C_0)\frac{\partial r_1}{\partial(\rho u)} + v\frac{\partial r_1}{\partial(\rho v)} &= 0 \\
C_0\frac{\partial r_2}{\partial(\rho v)} &= 0 \\
\frac{\partial r_3}{\partial \rho} + (u + C_0)\frac{\partial r_3}{\partial(\rho u)} + v\frac{\partial r_3}{\partial(\rho v)} &= 0.
\end{aligned}$$

These equations can be solved to yield

$$r_1 = u - C_0 \ln \rho, \quad r_2 = u, \quad r_3 = u + C_0 \ln \rho.$$

Hence we obtain the following approximations of u and ρ,

$$u = \frac{1}{3}\left(r_1 + r_2 + r_3\right), \quad \text{and} \quad \rho = \exp\left(\frac{r_3 - r_1}{2C_0}\right).$$

We can use these approximations at the exit to ensure that outgoing waves pass through and are not artificially reflected back. In the case $\lambda_1^F < 0$, $\lambda_2^F > 0$, $\lambda_3^F > 0$, r_1 represents the left moving waves and r_2 and r_3 the right moving waves. Thus we want to eliminate r_1 but allow r_2 and r_3 to pass through the boundary. This can be done by setting

$$r_1 = u^*_{M,j} - C_0 \ln \rho^*_{M,j}, \quad r_2 = u^n_{M-1,j} \quad \text{and} \quad r_3 = u^n_{M-1,j} + C_0 \ln \rho^n_{M-1,j},$$

where $u^*_{M,j}$ and $\rho^*_{M,j}$ are the initial values of u and ρ respectively.

4.6 Numerical Results

A series of numerical experiments were used to calibrate the model with the aim of determining an optimal set of parameter values that produced behaviour as close as possible to what we would physically expect. This involved varying the size of the room, the starting position of the crowd and the location of the exit. It was essentially a trial and error method but produced some intriguing results. In particular, it was found that the model was extremely sensitive to changes in the value of the anticipation coefficient C_0.

Figures 4.1 and 4.2 show the results for a $10m \times 10m$ room, with $C_0 = 0.4$, spatial step sizes $\Delta x = \Delta y = 0.2$ and a time step $\Delta t = 0.02$. Initially the crowd is gathered around the point $(3, 3)$ and the exit is positioned in the top right hand corner of the room between the points $y = 7$ and $y = 9$. The crowd remains tightly packed and slowly moves across the room reaching the exit at around $t = 10$. The density builds creating a pile up across the doorway, the crowd is unable to leave the room and density increases even further. The code runs up until a time of $t = 14.5$, after which problems arise at the boundary where unrealistically high density values mean that the scheme becomes unstable.

Figures 4.3, 4.4 and 4.5 show the effect of doubling the size of the anticipation coefficient to $C_0 = 0.8$. The same initial data, spatial and temporal step sizes were used. The behaviour of the crowd becomes very strange. Unlike in the above example, the crowd is much less densely packed and therefore moves more freely. After 4 seconds the shape of the crowd starts to become distorted and appears to move away from the exit towards the

bottom of the room. It was found that this distortion could be reduced slightly by decreasing both the space and time step lengths. Between $t = 8$ and $t = 10$ the crowd regains its composure and begins to move towards the exit. As above there is increase in density as the crowd starts to gather around the doorway. However, the initial spreading of the crowd means that these density values are much lower (although perhaps still slightly unrealistic) and actually start to decrease as the crowd filters through the exit.

Next, the effect of moving the exit to the bottom right hand corner of the room was investigated. The behaviour of the crowd became even more adverse. Initially the scheme was used both $C_0 = 0.4$ and $C_0 = 0.8$. The exit is located between the points $y = 2$ and $y = 4$ but in both cases the crowd heads towards the bottom of the room hitting the wall along the boundary at $y = 0$ (see Figures 4.6 and 4.7). With $C_0 = 0.4$ this initial distortion appears to be irreversible and the crowd moves randomly around the room with time. With $C_0 = 0.8$ the crowd moves around at the bottom wall before eventually correcting itself and reaching the exit at $t = 24$ (Figure 4.7). We have so far been unable to determine a value for C_0 that prevents this initial diversion, but the distortion can be decreased slightly by increasing C_0. However, if C_0 becomes too large the crowd distortions also start to appear on the upper boundary along $y = 10$. Figures 4.8 and 4.9 show the results for an anticipation coefficient of $C_0 = 1.3$. The high value of C_0 means that the scheme does not generate unphysical density values and our program runs much further forward in time. We are therefore able to observe the crowd as they gradually filter through the exit. By $t = 45$ most of the crowd has left

the room.

In general, the smaller the value of C_0 the greater the clustering effect and the higher the density. It appears that when $C_0 = 0.4$ the crowd moves too slowly through the doorway. Therefore a blockage occurs further restricting their movement and preventing an efficient exit. In section 4.2 we stated that the anticipation coefficient is related to pressure. If C_0 is low then the pressure is low and the magnitude of the wave speeds (λ_1, λ_3) are smaller. The slow speed of movement means that the crowd remains closely assembled and thus too many pedestrians reach the exit at the same time. Conversely, when C_0 is high the pressure is high and the waves travel much faster, dispersing the crowd and enabling the pedestrians to exit the room in an efficient manner. To maintain stability and prevent spurious solutions, these speeds need to be controlled via the time step Δt. One possibility would be to employ a variable time step. It appears from trials so far that when $C_0 = \textit{constant}$ there does not exist a value for which the two effects can be balanced. This suggests that a density dependent anticipation coefficient would perhaps be more adequate. The observed distortions may also be in part due to the dimensional splitting. A more effective scheme would be fully two dimensional.

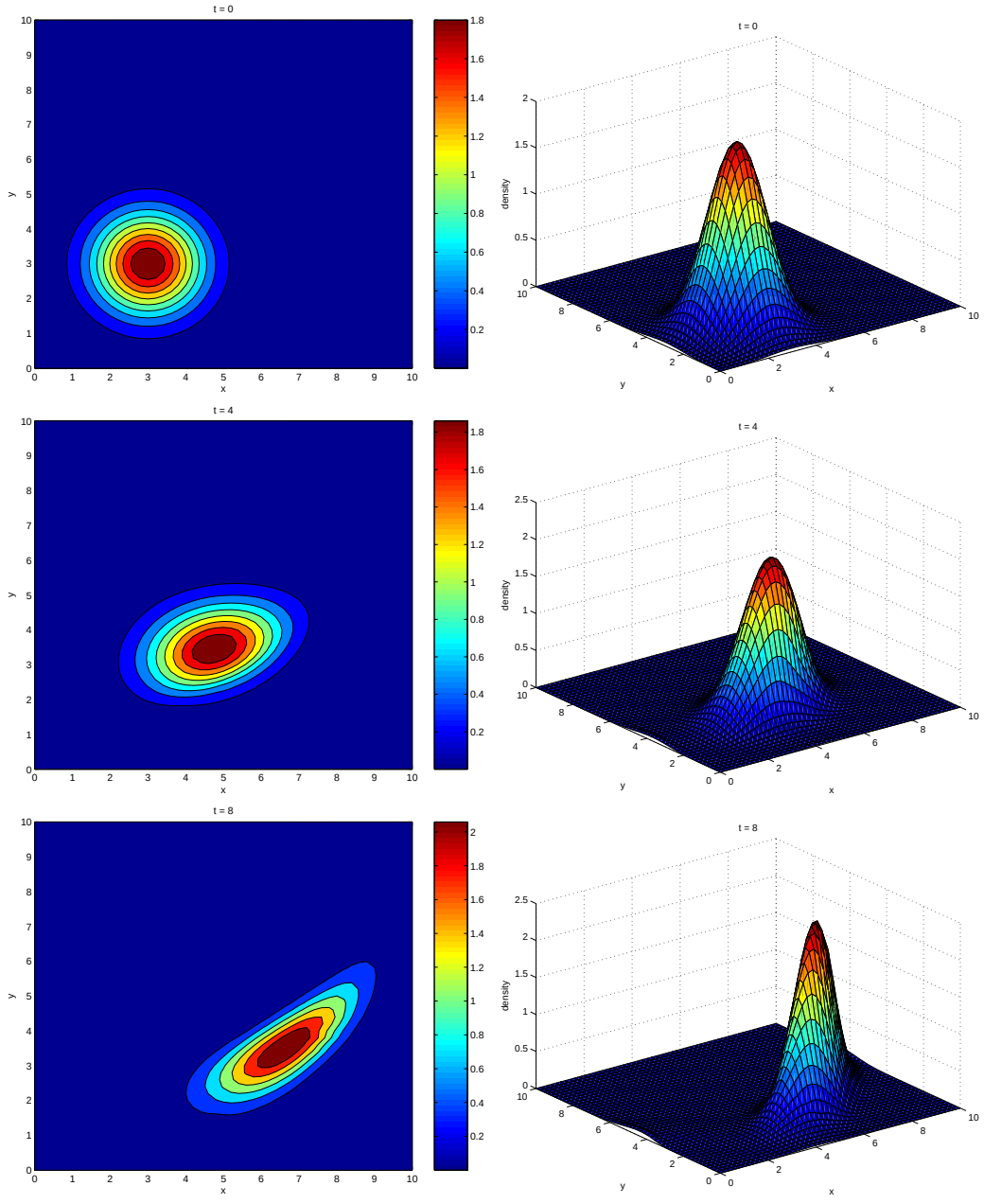

Figure 4.1: 2D crowd model - $10m \times 10m$ room with exit at $x = 10$, $7 \leq y \leq 9$, $C_0 = 0.4$, $\Delta x = \Delta y = 0.2$, $\Delta t = 0.02$.

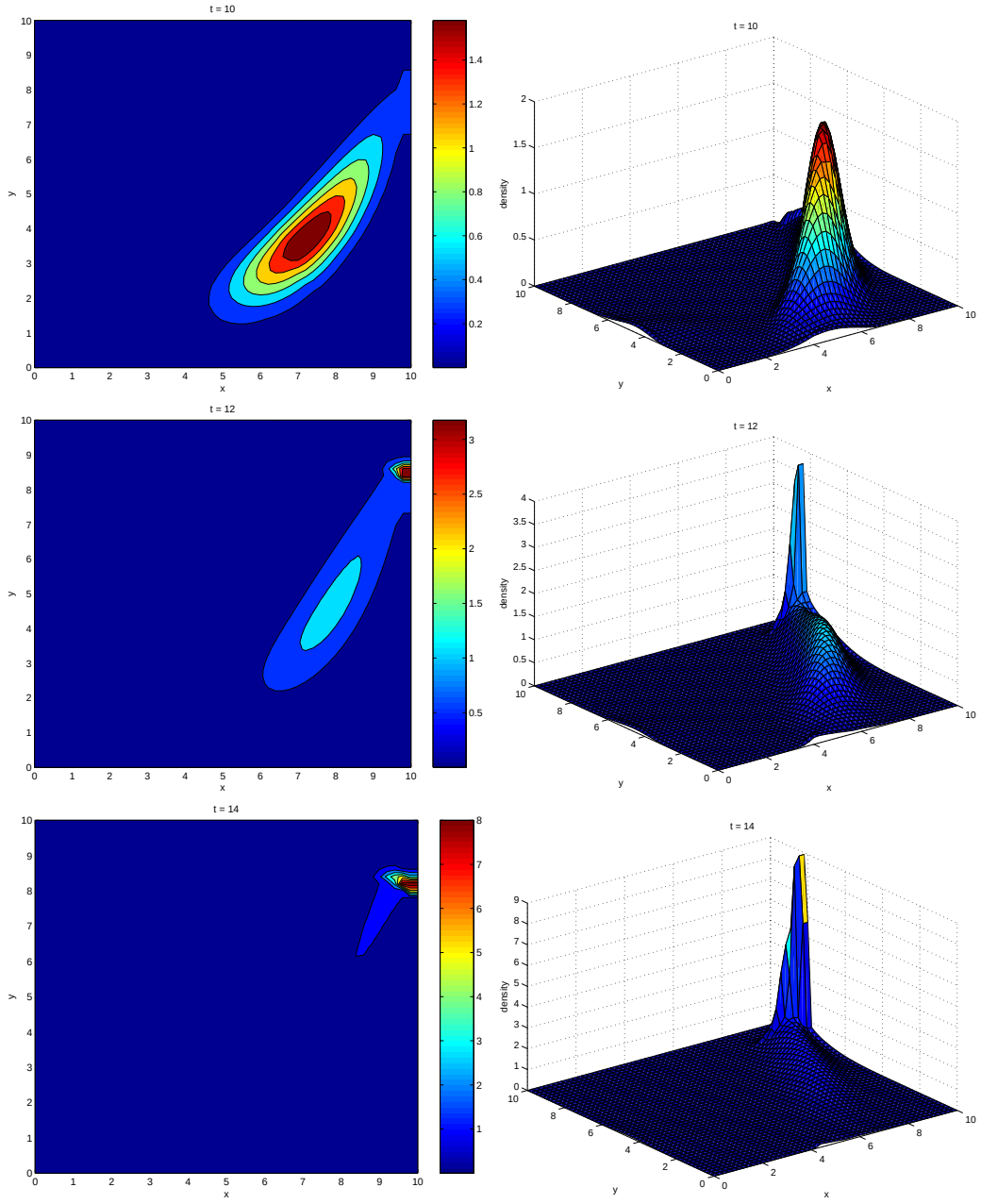

Figure 4.2: 2D crowd model - $10m \times 10m$ room with exit at $x = 10$, $7 \leq y \leq 9$, $C_0 = 0.4$, $\Delta x = \Delta y = 0.2$, $\Delta t = 0.02$.

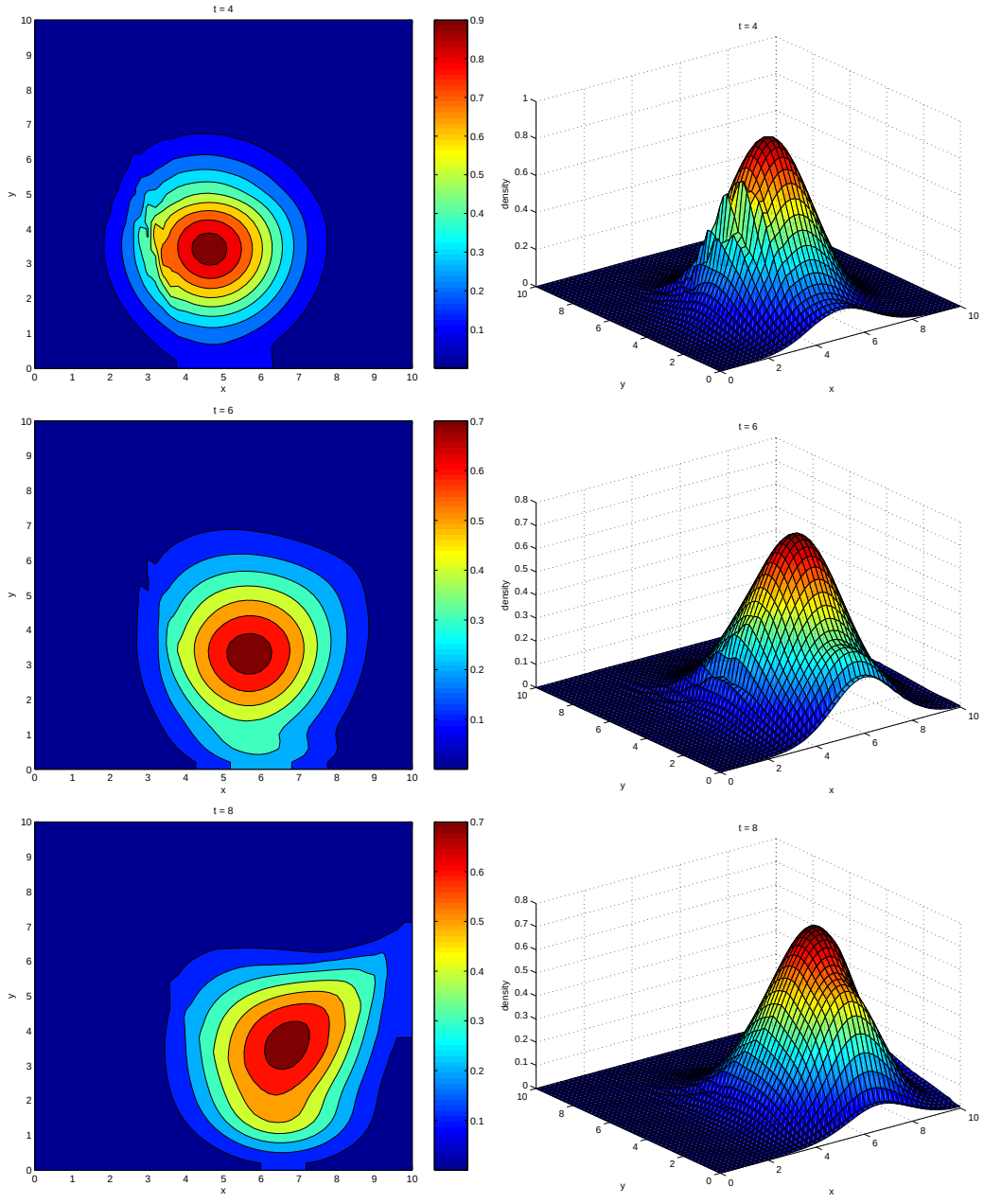

Figure 4.3: 2D crowd model - $10m \times 10m$ room with exit at $x = 10$, $7 \leq y \leq 9$, $C_0 = 0.8$, $\Delta x = \Delta y = 0.2$, $\Delta t = 0.02$.

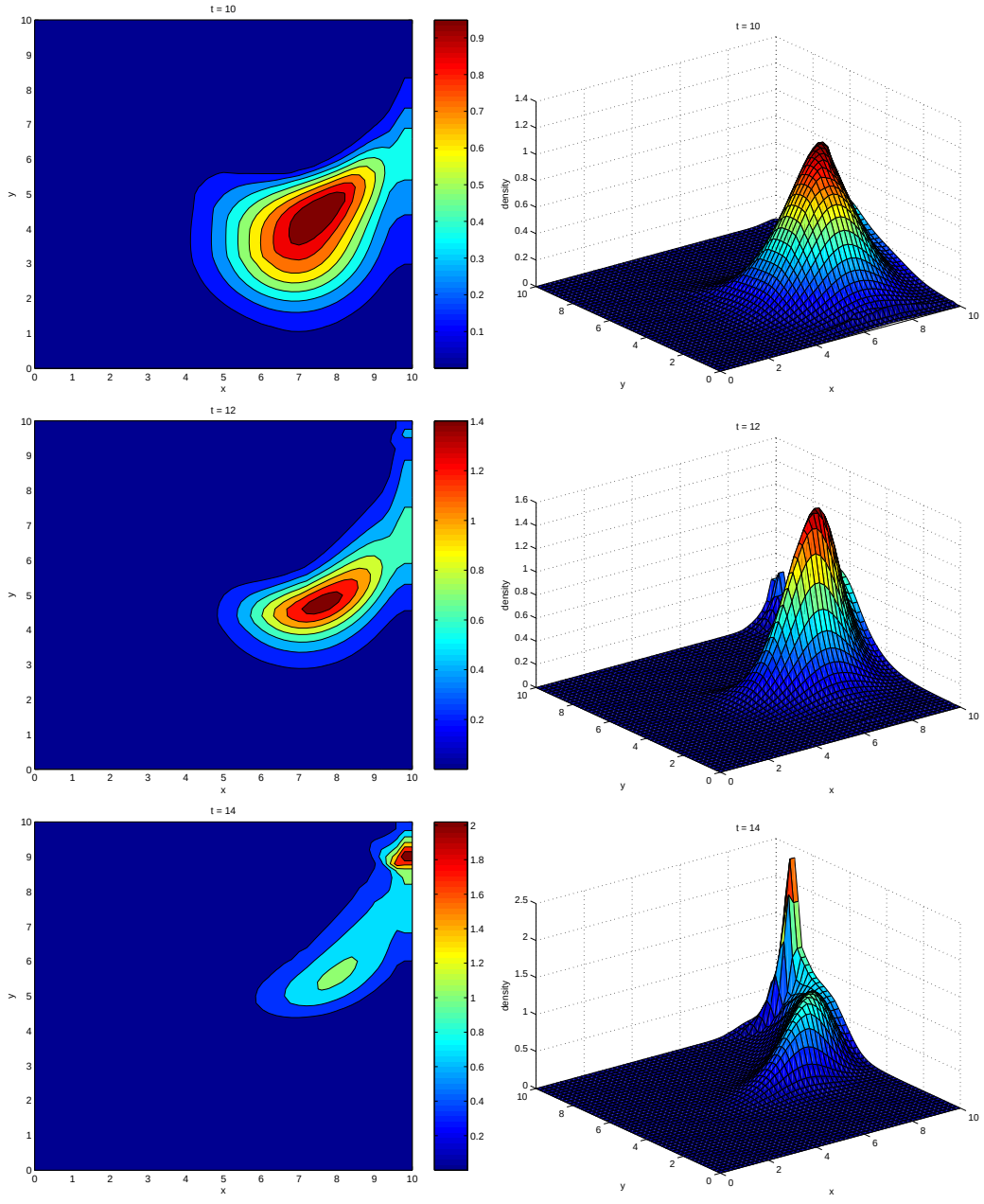

Figure 4.4: 2D crowd model - $10m \times 10m$ room with exit at $x = 10$, $7 \leq y \leq 9$, $C_0 = 0.8$, $\Delta x = \Delta y = 0.2$, $\Delta t = 0.02$.

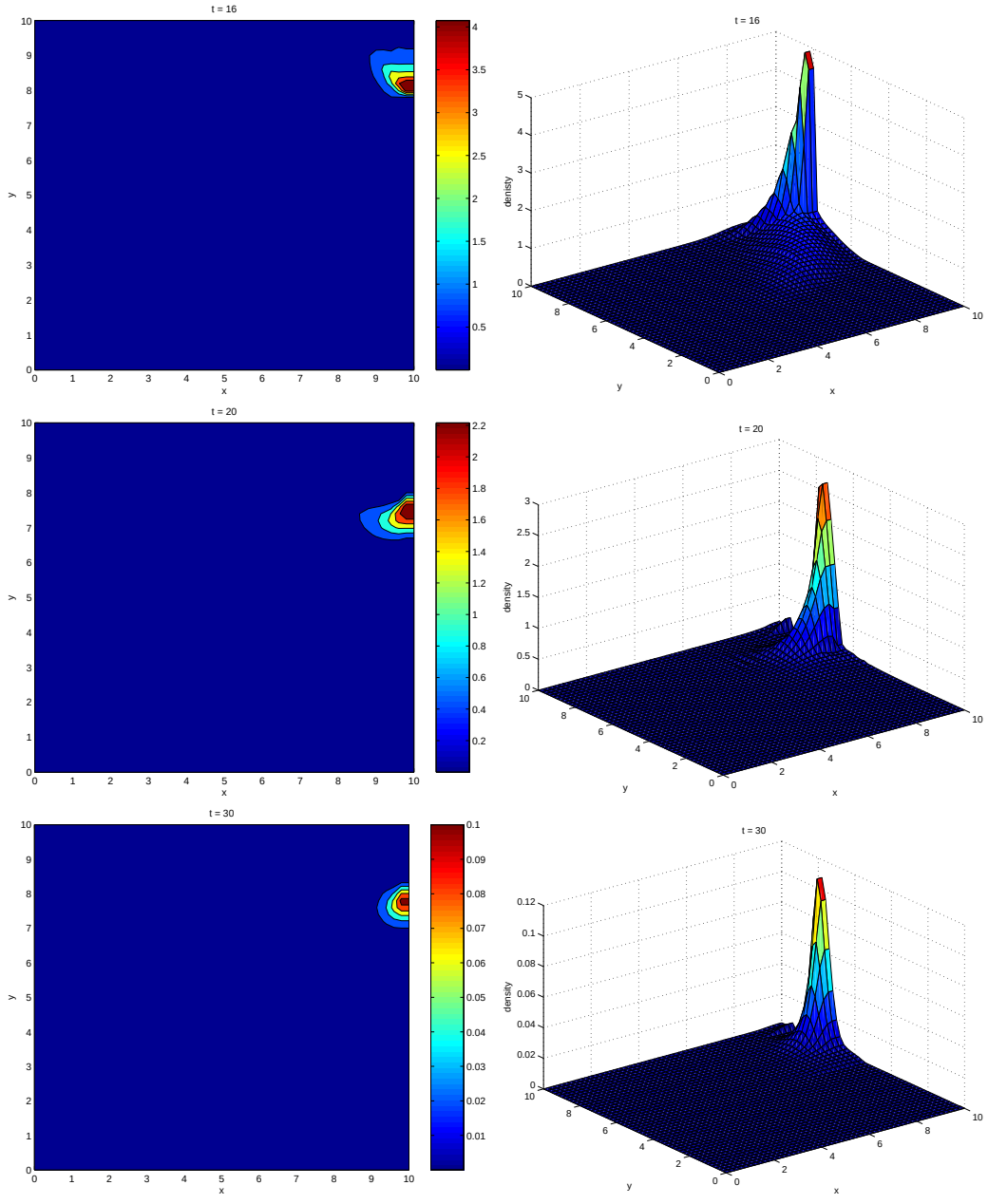

Figure 4.5: 2D crowd model - $10m \times 10m$ room with exit at $x = 10$, $7 \leq y \leq 9$, $C_0 = 0.8$, $\Delta x = \Delta y = 0.2$, $\Delta t = 0.02$.

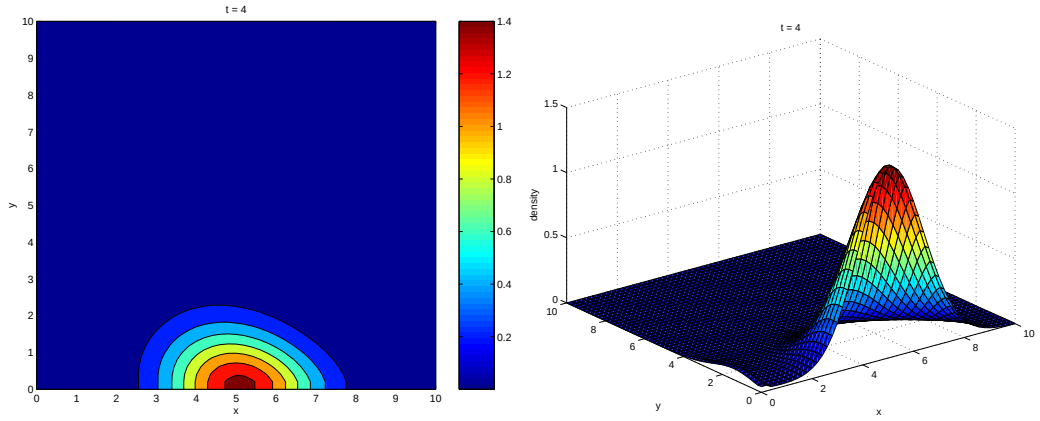

Figure 4.6: 2D crowd model - $10m \times 10m$ room with exit $x = 10$, $2 \leq y \leq 4$, $C_0 = 0.4$, $\Delta x = \Delta y = 0.2$, $\Delta t = 0.02$.

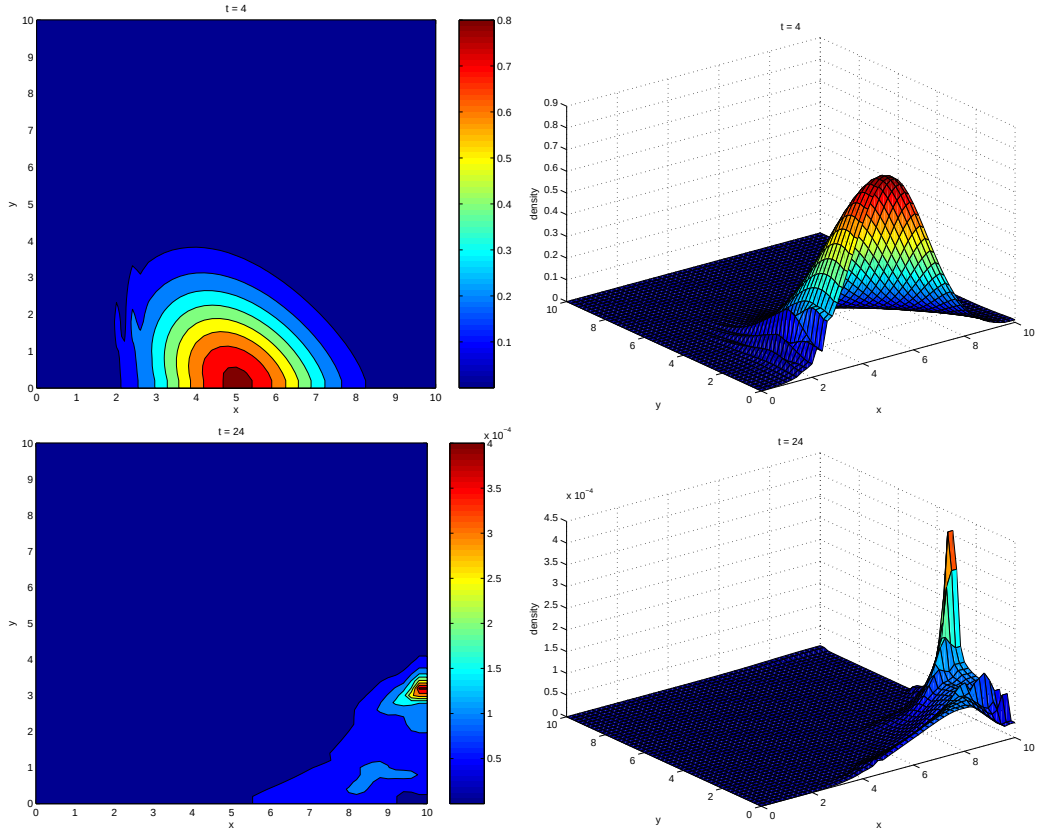

Figure 4.7: 2D crowd model - $10m \times 10m$ room with exit at $x = 10$, $2 \leq y \leq 4$, $C_0 = 0.8$, $\Delta x = \Delta y = 0.2$, $\Delta t = 0.02$.

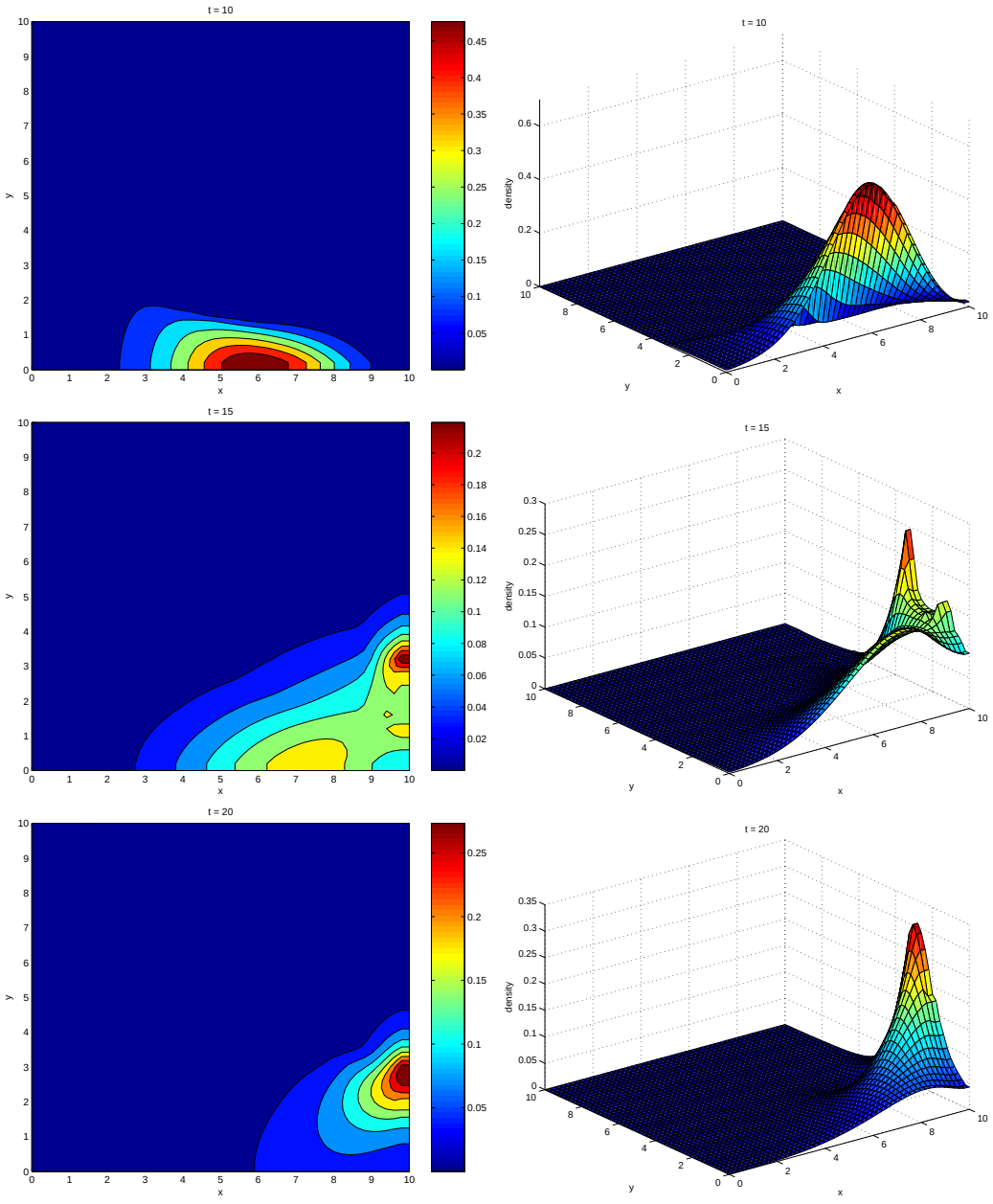

Figure 4.8: 2D crowd model - $10m \times 10m$ room with exit at $x = 10$, $2 \leq y \leq 4$, $C_0 = 1.3$, $\Delta x = \Delta y = 0.2$, $\Delta t = 0.02$.

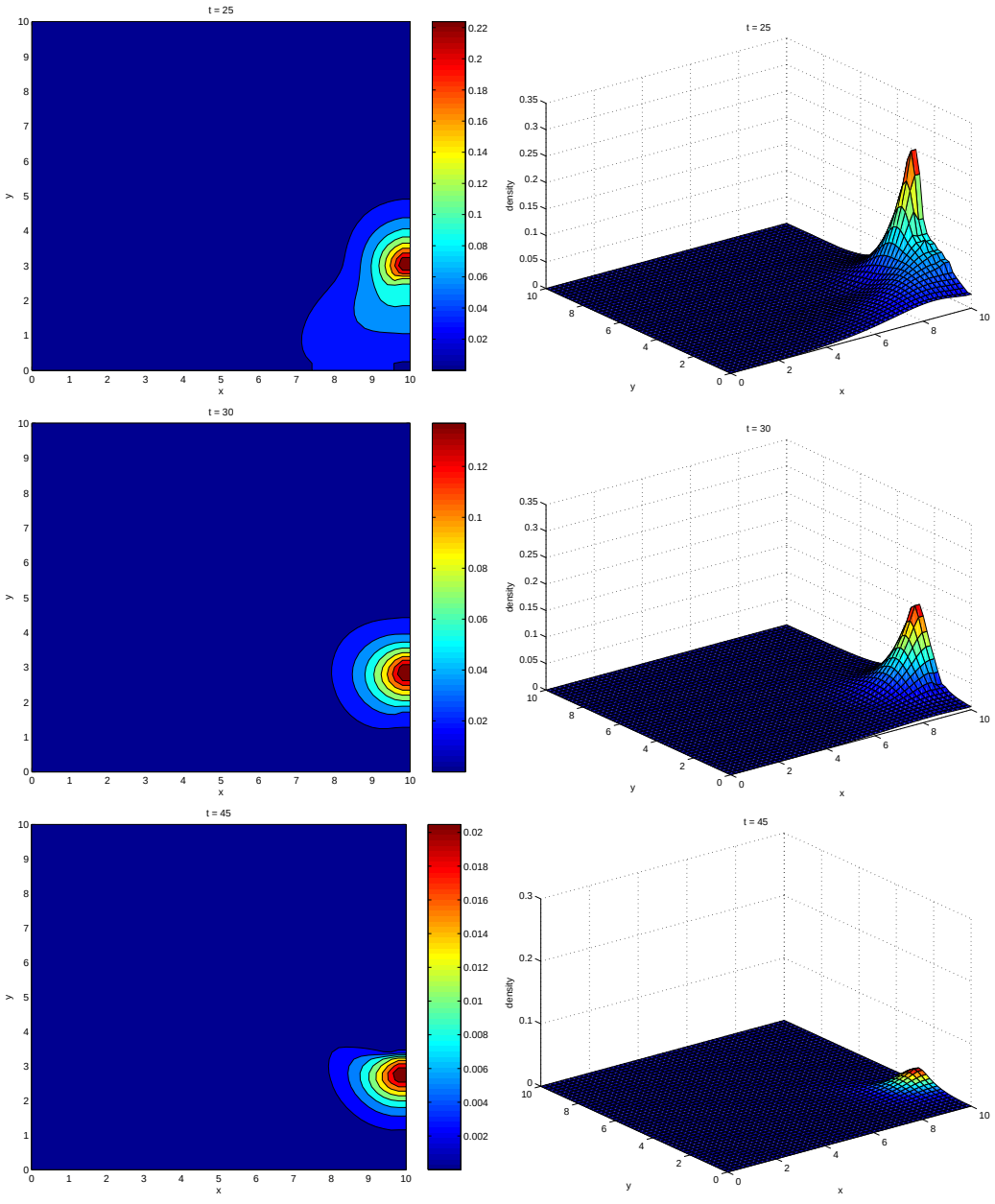

Figure 4.9: 2D crowd model - $10m \times 10m$ room with exit at $x = 10$, $2 \leq y \leq 4$, $C_0 = 1.3$, $\Delta x = \Delta y = 0.2$, $\Delta t = 0.02$.

Chapter 5

Conclusions and Further Work

The aim of this dissertation was to develop a numerical method for approximating two dimensional systems of hyperbolic conservation laws with source terms and then apply it to the variable depth shallow water equations and a macroscopic model of crowd flow. The technique of dimensional splitting was used to decompose the system of conservation laws into two parts that could be solved alternately in the x and y directions. We then adopted the Q scheme method of Bermúdez & Vázquez, using a two dimensional extension of Roe's Q scheme to numerically approximate the equations.

In chapter 3 we looked at the application of our method to the variable depth shallow water equations, first using a non-rotating Eulerian frame of reference and then extending the equations to include the effect of the Earth's rotation. This was done by adding a coriolis term to the source. The numerical solutions produced by the scheme were smooth and oscillation free. However, it was noted that the absence of any exact solutions made it difficult to fully appraise the accuracy of the method. We observed that the scheme suffered from dissipation leading to smearing of our numerical solution over

time. This could be lessened somewhat by refining the computational mesh but this consequently reduced the efficiency of the code. It was suggested that a better way of eliminating this diffusion would be to introduce a flux limiter which switches between a second order approximation when the region is smooth and a first order approximation near a discontinuity.

In chapter 4 we developed a two dimensional model of crowd flow from a one dimensional traffic flow model proposed by Payne and Whitham. A series of numerical trials were then used to evaluate the performance of the model. We then sought to interpret the resulting behaviour in terms of the pressure and wave speeds. It was found that the model was extremely sensitive to the value of the anticipation coefficient C_0. Under certain conditions the model did exhibit some attributes of crowd flow but a number of curious effects were produced. Computational errors were also experienced caused by the generation of unphysical density values, particularly near the boundaries.

Crowd dynamics is a vast and complex field and in this report we have barely touched on one aspect. The problem is not only multi-dimensional but also multi-faceted. The Payne Whitham model was originally developed for traffic and more work needs to be done to tune it to pedestrian flow. However, the approach is very simplistic and will never capture all the complex interactions required for a more realistic crowd flow model. In terms of the work undertaken so far, there is much room for improvement. Further analysis is required on stability, and finding a suitable anticipation coefficient C_0 that prevents the generation of unphysical density values and yields properties more akin to crowd flow. More generally, there remain numerous possibilities for further investigation, from simple changes to the

initial data and the structure of the domain of interest, such as including an entrance or multiple exits, to more advanced refinements, such as using a microscopic approach to allow for the psychological behaviour of humans, modelling individual preferences and physical interactions.

Bibliography

[1] A. Bermúdez & M.E. Vázquez, *Upwind methods for Hyperbolic Conservation Laws with Source Terms*. Computers and Fluids Vol. 23 No. 8, 1049 - 1071 (1994).

[2] A. Bermúdez & M.E. Vázquez, *Flux Vector and flux-difference splitting methods for the shallow water equations in a domain with variable depth*. Computer Modelling of Seas and Coastal Regions (Edited by P.W. Partridge), pp. 256 - 267, Computational Mechanics Publications Elsevier Applied Science, London (1992).

[3] A. Crossley, *Application of Roe's Scheme to the Shallow Water Equations on the Sphere*. MSc Dissertation, University of Reading (1994).

[4] P. Glaister, *Difference Schemes for the Shallow Water Equations*. Numerical Analysis Report 9/87, University of Reading (1987).

[5] E. Godlewski & P-A. Raviart, *Numerical Approximation of Hyperbolic Systems of Conservation Laws*. Applied Mathematical Sciences 118, Springer-Verlag, New York (1996).

[6] D. Helbing, *A Mathematical Model for the Behaviour of Pedestrians*. May 1998 (www.helbing.org).

[7] D. Helbing, *Models for Pedestrian Behaviour*. May 1998 (www.helbing.org).

[8] J. Hudson, *Numerical Techniques for the Shallow Water Equations*. Numerical Analysis Report 2/99, University of Reading (1999).

[9] J. Hudson, *Numerical Techniques for Morphodynamic Modelling*. PhD Thesis, University of Reading (2001).

[10] P. Marno, *Crowded - Macroscopic and Microscopic Models for Pedestrian Dynamics*. Numerical Analysis Report 4/2002, University of Reading (2002).

[11] R. McIlveen, *Fundamentals of Weather and Climate*. Nelson Thornes Ltd. (2003)

[12] J.V. Morgan, *Numerical Methods for Macroscopic Traffic Models*. PhD Thesis, University of Reading (2002).

[13] P.L. Roe, *Approximate Riemann Solvers, Parameter Vectors, and Difference Schemes*. J. Comput. Phys. Vol. 43, 357 - 372 (1981).

[14] C.G. Rossby et al, J. Marine Research Vol. 2, 38, (1939).

[15] G. Strang, *On the Construction and Comparison of Difference Schemes*. SIAM J. Num. Anal. Vol. 5, 506 - 517 (1968).

[16] P.K. Sweby, *High Resolution Schemes using Flux Limiters for Hyperbolic Conservation Laws*. SIAM J. Num. Anal. Vol 21 No.5, 995 - 1011 (1984).

[17] W.M. Thacker, *Some exact solutions to the nonlinear shallow-water wave equations*. J. Fluid Mech. Vol. 107, 499 - 508 (1981).

[18] R.J LeVeque, *Numerical Methods for Conservation Laws*. Birkhäuser-Verlag (1992).

[19] G.B. Whitham, *Linear and Nonlinear Waves*. John Wiley, New York (1974).

[20] N.N Yanenko, *The Method of Fractional Steps*. Springer-Verlag, New York, (1971).

[21] H.M. Zhang, *A finite difference approximation of a non-equilibrium traffic flow model*. Transp. Res. B 35, 337 - 365 (2001).

[22] H.M. Zhang, *New Perspectives on Continuum Traffic Flow Models*. Networks and Spatial Economics 1, 9 - 33 (2001).